ÉCOLE POLYTECHNIQUE
FÉDÉRALE DE LAUSANNE

Jeannette Liniger

Muscles in a Shoulder Model:

Identification of the necessary number of muscle cables

Semester Project

Laboratory of Biomechanical Orthopedics
Swiss Federal Institute of Technology Lausanne

Supervision

Christoph Engelhardt
Alexandre Terrier
Prof. Dominique Pioletti

June 2014

Contents

Chapter 1

Introduction

The shoulder complex is an important and complex system of the human body. It consists of several bones and joints and is moved and stabilized by 16 muscles. The movement of the human shoulder is the result of a complex coordination of bony articulations and muscle forces. The shoulder must be mobile to allow the great range of motion necessary for the hands and arms. At the same time it must be stable enough to allow fast dynamic movements and bear external loads.

This balance between stability and mobility makes the shoulder complex an interesting field of research. Several experimental and numerical studies have already been done to assess movement patterns, muscle coordination and joint loads in the shoulder. While experimental in vivo studies assure to be close to reality, numerical studies have the advantage of being independent of specimens, they allow to measure experimentally not accessible quantities. Furthermore, a model permits to simulate certain movements and provides a better understanding of the shoulder complex. Finally, the results from these numerical studies help to find treatments for pathologies.

The existing numerical model of the shoulder complex can compute the muscle forces necessary for a given movement. A solver was developed that uses inverse dynamics and nullspace optimization to compute the muscle forces. The muscle segments in the shoulder are modelled as cables. In the existing model one cable is implemented per muscle segment. However, the 1D modelling of a muscle segment represents a great simplification of the muscle. When modelling the muscle as 1D, the fibrous structure of a muscle is not represented. Furthermore, the interaction between different muscles is not taken into account and the distribution of the stress in the muscle cannot be modelled. The numerical study with one cable per segment is therefore not representative. To have a better approximation of a muscle, multiple cables per muscle segment have to be implemented. Then the minimal necessary number of cables to get consistent forces can be determined.

The project's aim is to adapt the existing model and introduce the parametrization of the number of cables. The first part of the report introduces the most important aspects of the shoulder complex anatomy. The joint coordinates necessary are introduced as well as the standardized joint motion in the shoulder. To better understand the methods used for the numerical model the basics of kinematic and dynamic modelling necessary to estimate the muscle forces are presented. The second part shows the methods used to introduce multiple cables per muscle segment in the model. The third part contains a comparison between the two methods and the results of the numerical studies. These results are then discussed, a conclusion is drawn and the report is finished with an outlook.

Chapter 2

State of the Art

In the first part the anatomy of the shoulder is presented. Especially the shoulder complex muscles' origin and insertion areas are shown. Then the joint coordinate systems (JCS) used in the model are defined. In the second part an introduction to the kinematic and dynamic modelling theory as well as the muscle force estimation is given. The last part consists in a brief review of some geometric principals.

2.1   Anatomy of the Shoulder Complex

2.1.1   Bones and Joints

The human skeletal system is made up of 206 bones. The skeleton's purpose is to protect the body's major organs and to allow motion and force transmission. A bone is composed of two types of tissue, cortical and trabecular bone. For a long bone, the trabecular bone tissue is located at the ends of the bone and in its center. The trabecular bone has a spongy structure, which allows a good distribution of the loads. The cortical bone forms the walls of the central part of the bone. It is more dense and can take high constraints. The bones form joints with each other to allow movement. At the joint interfaces cartilage reduces the friction in the joint. The bones are held together by ligaments. (Pioletti, 2013) The main bones in the shoulder are the humerus (upper arm bone), the scapula (shoulder blade) and the clavicle (collarbone) (cf. Figure 2.1).
The humerus is the longest bone of the upper extremities. In the section closest to the shoulder joint the head, a spheroid ariculation surface, and the greater and lesser tuberosity are located. The tuberosity serves as an attachment site for both ligaments and tendons. The scapula is a thin triangular bone lying on the posterior side of the thorax. The scapula has several processes: The coracoid, spine, acromion and glenoid process. These processes serve as both origin and insertion site for multiple muscles. The clavicle connects the trunk to the other bones in the shoulder . The bone has a double curve along its long axis. It also serves as a site for muscle attachment as well as for protection of underlying neurovascular structures. (Terry and Chopp, 2000)

These three bones are integrated into the skeleton of the trunk, meaning the sternum, the rips and the vertebra. This construct can be seen in Figure 2.2. In this project the assembly of these bones is called shoulder complex.
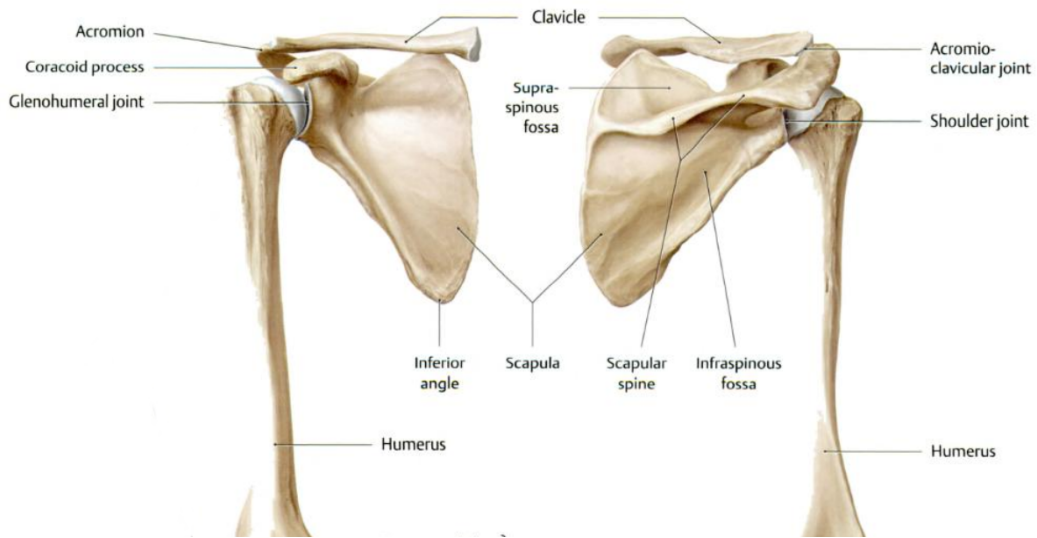
Figure 2.1: The bones of the shoulder joint (Schuenke et al., 2010)
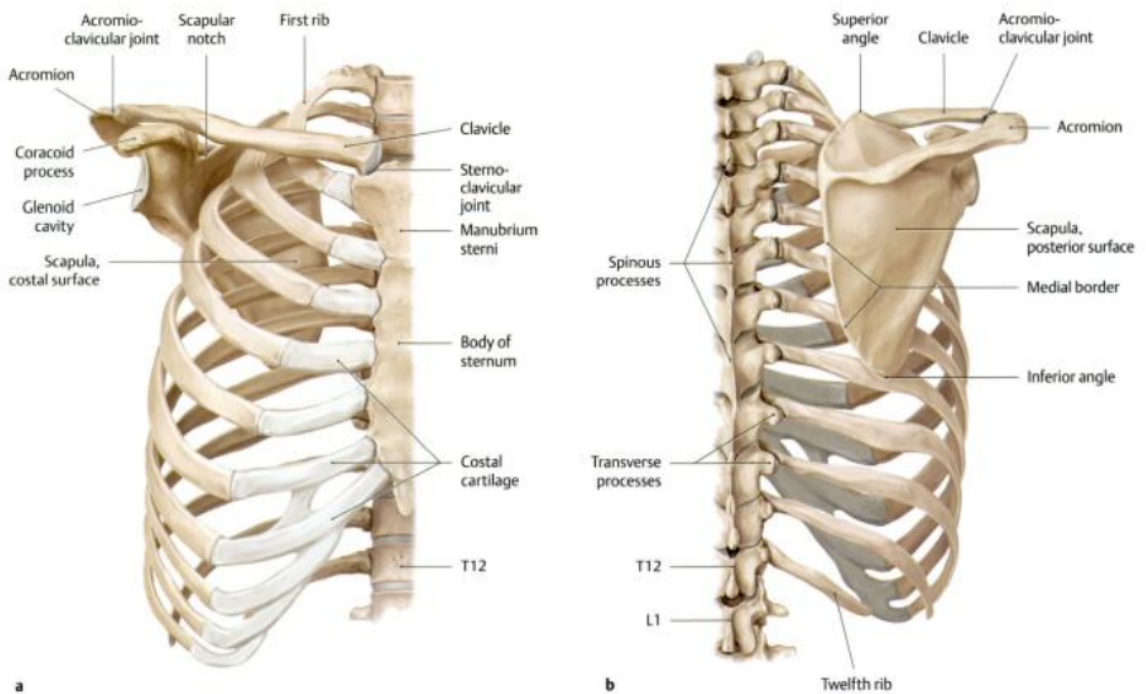

Figure 2.2: Integration of the shoulder bones into the trunk skeleton (Schuenke et al., 2010)

Bones of the shoulder complex are linked by several joints. The major joint is the gleno-humeral joint, which is mostly referred to as the shoulder joint. It is a synovial ball and socket joint and involves articulation between the proximal head of the humerus and a shallow socket in the scapula called glenoid fossa (more commonly glenoid cavity). Due to the small joint socket the shoulder is a very mobile joint. However, due to the same reason the stability in the shoulder can be an issue. (Terry and Chopp, 2000)

There are further joints in the shoulder complex, such as the sternoclavicular joint between the sternum and the clavicle and the acromioclavicular joint between the acromion, a continuation of the scapular spine, and the clavicle. Furthermore, there is the scapula-thoracic joint between the scapula and the thorax.

2.1.2 Muscles

The muscles are the engine of the musculoskeletal system. Muscles generate force, stiffen the joints, move and thermoregulate the human body. They can be seen as a machine that converts chemical energy into mechanical work as well as heat. Skeletal muscles account for approximately 40% of the body weight and are thus the largest organ of the body. Generally, a tendon attaches the muscle to the bone. (Pioletti, 2013)

The shoulder complex is spanned by 16 muscles. The shoulder muscles can be categorised with a compromise between topographical and functional considerations. The shoulder joint muscles are defined as the muscles that span over the glenohumeral joint, including the rotator cuff muscles as well as the more superficial muscles. The complete list can be seen in Table 2.1. The rest are muscles that have migrated from the trunk (cf. Table 2.2). All of these muscles belong to the previously defined shoulder complex.

1. Muscles of the shoulder joint
Posterior muscle group
Supraspinatus (rotator cuff)
Infraspinatus (rotator cuff)
Teres minor (rotator cuff)
Subscapularis (rotator cuff)
Deltoid
Latissimus dorsi
Teres major
Anterior muscle group
Pectoralis major
Coracobrachialis

Table 2.1: Functional-topographical classification of shoulder muscles (Schuenke et al., 2010)

2. Muscles migrated from the trunk
Shoulder muscles that have migrated from the head
Trapezius
Posterior muscles of the trunk and shoulder
Rhomboid major
Rhomboid minor
Levator scapulae
Anterior muscles of the trunk and shoulder
Subclavius
Pectoralis minor
Serratus anterior

Table 2.2: Functional-topographical classification of shoulder muscles (Schuenke et al., 2010)

Origin and insertion

Every muscle has an origin and an insertion area. The origin of a muscle is the point of attachment that remains relatively fixed during contraction. The muscle inserts on to the bone that is moved by the contraction of the muscle. For the 16 muscles of interest a comprehensive table is in Appendix A where the origin and insertion as well as their main function is specified.

Rotator cuff muscles

The rotator cuff is a group of deep muscles in the shoulder complex. The rotator cuff consists of four muscles: The teres minor, the infraspinatus, the supraspinatus and the subscapularis muscle. The four muscles origin from the scapula and insert into the humeral head (cf. Figure 2.3). The function of the rotator cuff muscles is to stabilize the glenohumeral joint. The muscles hold the humeral head in the glenoid cavity (Hansen, 2010).
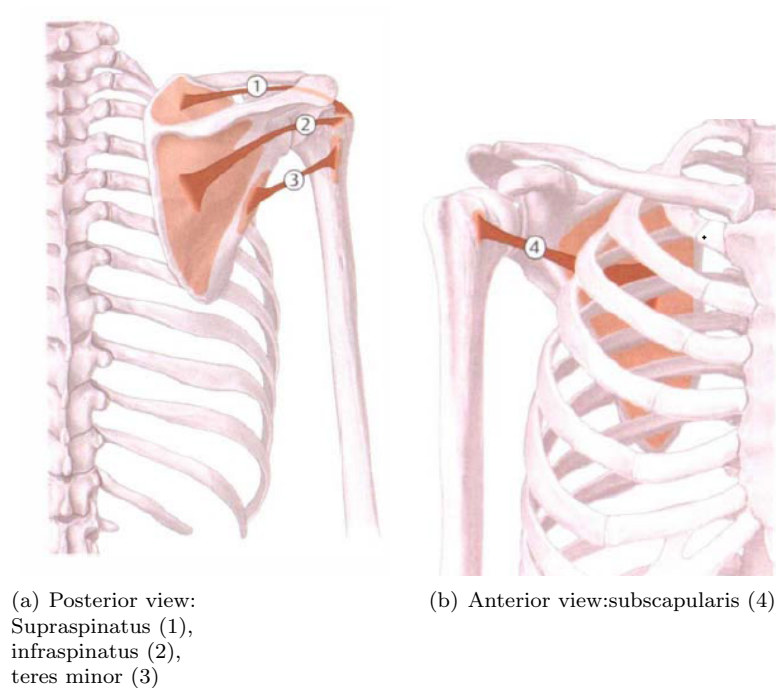

(a) Posterior view:
Supraspinatus (1),
infraspinatus (2),
teres minor (3)

(b) Anterior view:subscapularis (4)

Figure 2.3: Origin and insertion of the rotator cuff muscles (Schuenke et al., 2010)

Deltoid muscle

The deltoid is a superficial muscle in the shoulder complex that gives the shoulder its rounded form. The muscle has three sections, an anterior part, a medial part and a posterior part. They originate from three different locations, the clavicle, the acromial process and the scapular spine respectively. They insert all together into the deltoid tuberosity of the humerus. (Terry and Chopp, 2000)

The deltoid muscle moves the shoulder joint. The middle part is responsible for the abduction of the arm at the shoulder. The anterior part flexes and medially rotates the arm and the posterior part extends and laterally rotates the arm at shoulder. (Hansen, 2010)

Figure 2.4: Deltoid muscle: Anterior (1), medial (2), posterior (3) (Schuenke et al., 2010)

2.2   Anatomical Reconstruction

An anatomical reconstruction is used to reconstruct a biological form, such as bones or muscles. An anatomical reconstruction can be done using different data sources such as computed tomography (CT) or Magnetic Resonance Imaging (MRI). The MRI or CT scans contain cross sectional images of the tissue. These images are segmented one by one to highlight the 3D anatomical structures. A software, such as Amira, is necessary to visualise the segmented data. Amira is 3D software platform for visualisation, manipulation and understanding data from different imaging modalities. For more detail on the Amira software refer to Amira online (May 2014).

2.3   Kinematic Modelling

Kinematics describes the motion of objects. The kinematics of a multi-link system specifies the position, speed and acceleration of the reference frame of a segment. A map to describe these transformations has to be calculated, which is called the kinematic model (Burri and Bleuler, 2013).

2.3.1   Definitions

Kinematic chain

A kinematic chain is an assembly of rigid bodies linked together by joints. The Figure 2.5 shows a chain with two segments (L1 and L2) and two joints.
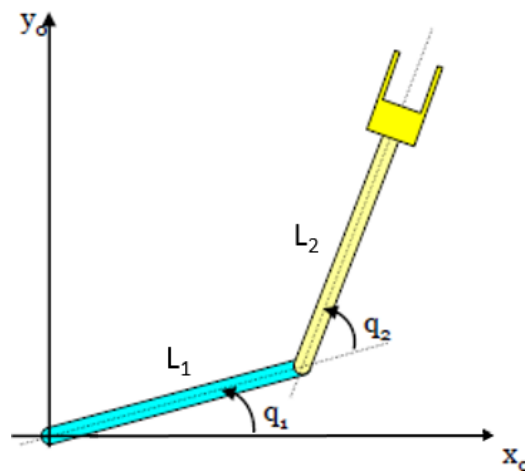
Figure 2.5: A simple kinematic chain (Burri and Bleuler, 2013)

Generalized coordinates

A set of generalized coordinates, also called joint variables, describe the joint space. They describe the displacement of the reference frames of the segments (position or angle). These variables are commonly represented by q (cf. Figure 2.5). The speed and the acceleration are noted respectively $\dot{q}(t)$ and $\ddot{q}(t)$. There is one generalized coordinate per degree of freedom (DOF) of the chain.

Operational coordinates

The operational coordinates describe what the end-effector of the kinematic chain does in the world reference frame. If the world reference is in Cartesian coordinates the operational coordinates are (x, y, z).

Kinematic models

The purpose of the kinematic model, also called geometric model, is to establish the link between the joint variables and the operational coordinates. It provides the mathematical tools to transform from one set of variables to the other.

The forward kinematic model, also direct geometric model, is a set of kinematic equations. These equations compute the position of the end-effector in the world reference frame from the generalized coordinates. In other words, they express the operational coordinates (x, y, z) as a function of the generalized coordinates $(q_1, q_2, ..., q_n)$ (cf. Figure 2.6).
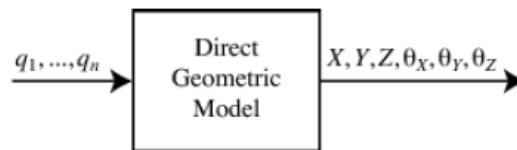
Figure 2.6: Forward kinematics (Burri and Bleuler, 2013)

Inverse kinematics, also inverse geometric model, uses the kinematic equations to determine the generalized coordinates that provide a desired position of the end-effector in the world reference frame. Hence, express the generalized coordinates $(q_1, q_2, ..., q_n)$ as a function of the operational coordinates (x, y, z) (cf. Figure 2.7).
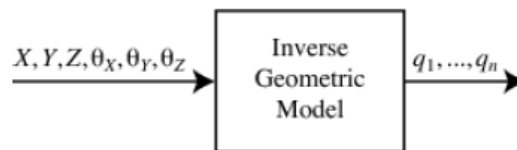

Figure 2.7: Inverse kinematics (Burri and Bleuler, 2013)

2.3.2 Joint Coordinate System for the Shoulder Complex

In order to standardize the description of joint motion the Society of Biomechanics (ISB) has proposed a set of local coordinate systems (LCS). The following section gives a brief review of this standardized description, for more detail refer to Wu et al. (2005): First a set of bony landmarks for the shoulder complex was defined (cf. Table 2.3).

Thorax	C7:	Spinous process of the 7th cervical vertebra
	T8:	Spinal porcess of the 8th thoracic vertebra
	IJ:	Deepest point of suprasternal notch
	PX:	Xiphoid process, most caudal point on the sternum
Clavicle	SC:	Most ventral point on the sternoclavicular joint
	AC:	Most dorsal point on the acromioclavicular joint (shared with the scapula)
Scapula	TS:	Root of the spine, midpoint of the triangular surface on medial border of the scapula in line with the scapular spine
	AI:	Inferior angle, most caudal point of the scapula
	AA:	Acromial angle, most laterodorsal point of the scapula
	PC:	Most ventral point of processus coracoideus
Humerus	GH:	Glenohumeral rotation center, estimated by regression or motion recordings
	EL:	Most caudal point on lateral epicondyle
	EM:	Most caudal point on medial epicondyle

Table 2.3: Anatomical landmarks: Thorax, clavicle, scapula and humerus. (Wu et al., 2005)

The next step is to define the coordinate system per body segment, here for the thorax, the clavicle, the scapula and the humerus (cf. Table 2.4).

With these local coordinate systems the motion of the shoulder joint can be described. To standardize the motion of the shoulder, it was decided that Euler angles should be used to describe all rotations. The proposed standardization suggests that the coordinate systems of the proximal and distal body segment in question are initially aligned to each other. This alignment is obtained by the introduction of anatomical orientations of these coordinate systems. When a rotation occurs, the rotation of the distal coordinate system should be reported with respect to the proximal coordinate system. If both coordinate systems are aligned the standardized sequence of rotation is the following: the first rotation around one of the common axes, the second rotation around the axis of the moving coordinate system and the third around a rotated axis of the moving coordinate system. To describe the joint displacement, a common point in both the distal and proximal coordinate systems should be taken. Such a point could be for example the initial rotation center. To represent true joint motion, the displacement should be described with respect to the axes of the coordinate system of the segment directly proximal to the moving segment. (Wu et al., 2005)
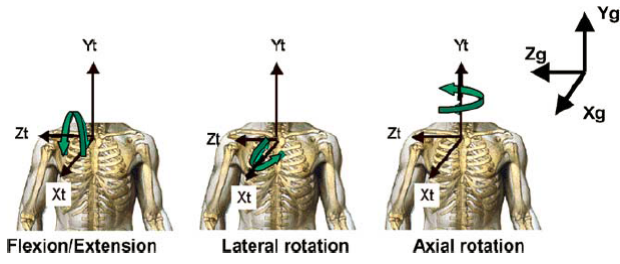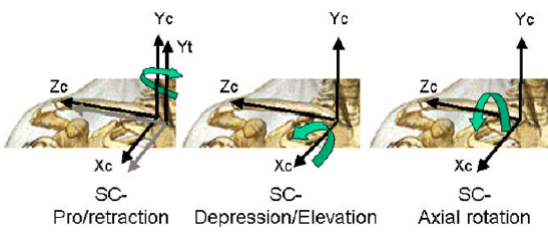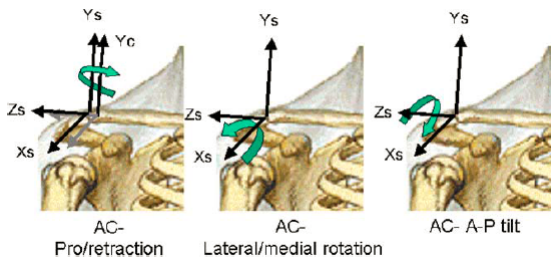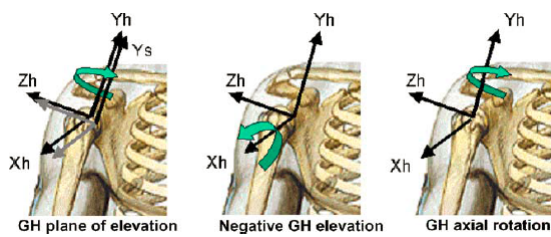
Thorax coordinate system - $X_t Y_t Z_t$

O_t:	The origin coincident with IJ.	
Y_t:	The line connecting the midpoint between PX and T8 and the midpoint between IJ and C7, pointing upwards.	
Z_t:	The line perpendicular to the plane formed by IJ,C7 and the midpoint between PX and T8, pointing to the right.	
X_t:	The common line perpendicular to the Z_t and Y_t axis, pointing forwards.	

Clavicle coordinate system - $X_c Y_c Z_c$

O_c:	The origin coincident with SC.
Z_c:	The line connecting SC and AC, pointing to AC.
X_c:	The line perpendicular to Z_c and Y_t, pointing forward. Note that the X_c-axis is defined with respect to the vertical axis for the thorax(Y_t-axis) because only two bony landmarks can be discerned at the clavicle.

Scapula coordinate system - $X_s Y_s Z_s$

O_s:	The origin coincident with AA.
Z_s:	The line connecting TS and AA, pointing to AA.
Y_s:	The line perpendicular to the plane formed by AI, AA, and TS, pointing forward. Note that because of the use of AA instead of AC, this plane is not the same as the visual plane of the scapula bone.
Y_s:	The common line perpendicular to the X_s- and Z_s- axis, pointing upwards.

Humerus coordinate system - $X_h Y_h Z_h$

O_h:	The origin coincident with GH.
Y_h:	The line connecting GH and the midpoint of EL and EM, pointing to GH.
X_h:	The line perpendicular to the plane formed by EL, EM, and GH, pointing forward.
Z_h:	The common line perpendicular to the Y_h- and Z_h-axis, pointing to the right.

Table 2.4: Local coordinate systems for the shoulder complex. (Wu et al., 2005)

2.3.3   Kinematic Model of the Shoulder Complex

In biomechanics, kinematics can be used to describe the motion of the human skeleton. The human skeleton can be seen as segments linked together by different joints. In the human body different kinds of joints exist with varying degrees of freedom (DOF).

In the following section a brief review of the kinematic model of the shoulder complex is presented, for more detail please refer to Ingram et al. (2012). When building the kinematic chain of the shoulder complex the segments considered are the thorax, the clavicle, the scapula and the humerus. The segments are linked through the sternoclavicular joint (SC), the acromioclavicular joint (AC) and the glenohumeral joint (GH). For the general model each of these joints is considered as an ideal spherical joint with three DOF. The last joint to consider is the scapulo-thoracic joint (ST), which is modelled using point-to-surface-constraints. With these assumptions the kinematic chain has a total of 7 DOF.

To build the kinematic model, the joint coordinates as well as the reference frames for the segments have to be defined. The standardized definition described in Section 2.3.2 is used.

The Figure 2.8 shows the shoulder complex with the kinematic chain, the bony landmarks, the joint reference system and coordinates. The notation used for the local origin and reference system is O^i, e_1^i, e_2^i, e_3^i, with the indices $i = t, c, s, h$ for thorax, clavicle, scapula and humerus. The absolute reference frame is placed at IJ.
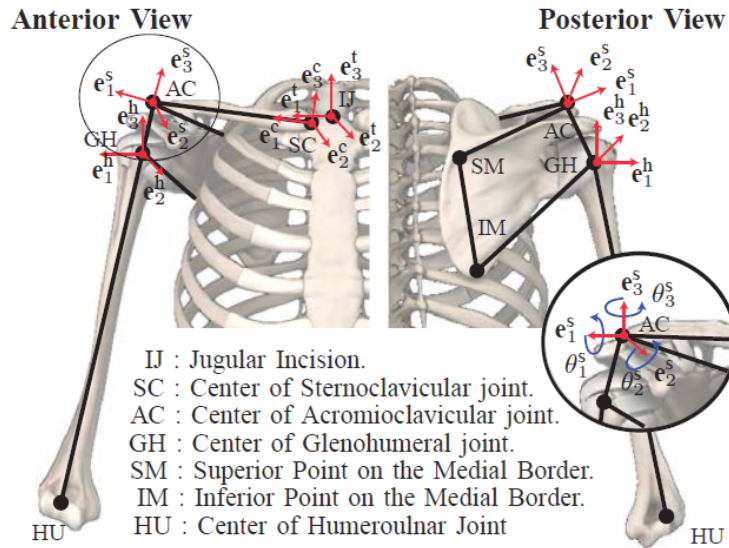

Figure 2.8: The Shoulder complex:Kinematic chain and the JCS (Ingram et al., 2012)

In the zoomed detail in Figure 2.8 the rotations around the reference system at the AC joint are shown. To describe these rotations a vector of three coordinates for each segment is used:

$$\mathbf{x_i} = (\theta_1^i \; \theta_2^i \; \theta_3^i) \; \in \; \chi_i \subset \mathbb{R}^3 \quad i = t, c, s, h \tag{2.1}$$

These are the generalized coordinates and χ_i is the bone configuration space.

A point on a bone or segment can be described as:

$$\mathbf{p_i} = (p_2^i \; p_2^i \; p_3^i) \; \in \; \mathcal{W}_i \subset \mathbb{R}^3 \quad i = t, c, s, h \tag{2.2}$$

The workspace $\mathcal{W}$ attributed to each bone is equal to the cartesian coordinate space of the local reference frame. In order to be able to compute a point p_i in the absolute workspace a set of maps has to be defined:

$$\begin{aligned} \xi_j \ : \ & \mathcal{W}_j \rightarrow \mathcal{W}_t \\ & \mathbf{P_j} \rightarrow \xi_j(p_j) = \mathbf{R_j p_j}, \quad j = c, s, h \end{aligned} \qquad (2.3)$$

The rotation matrix R_j is constructed using the joint coordinates. This set of equations is the forward kinematic model for the shoulder complex. The inverse model is described by the inverse of this map.

2.4 Dynamic Modelling

The dynamic modelling of a multi-link system describes the effects of external forces or torques on the motion of a body. The dynamic model is calculated using either the Newton-Euler or the Lagrangian approach (Burri and Bleuler, 2013).

2.4.1 Definitions

Generalized forces

A generalized force is associated with each generalized coordinate defined earlier. They can be either forces or torques and are denoted $\Gamma(t)$.

Dynamic models

The direct dynamic model describes the position, speed and acceleration of the end-effector as a function of the generalized forces in the system, $q(t) = f_D(\Gamma(t))$ (cf. Figure 2.9).
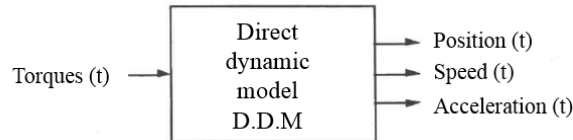

Figure 2.9: Direct dynamic model (Burri and Bleuler, 2013)

The inverse dynmamic model is used to compute the torques necessary to reach a certain position, speed and acceleration of the end-effector, $\Gamma(t) = f_I(q, \dot{q}, \ddot{q})$ (cf. Figure 2.10).
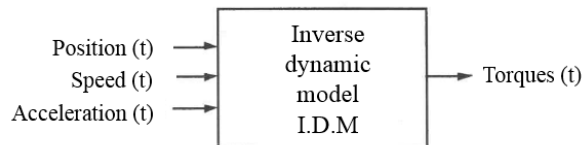

Figure 2.10: Inverse dynamic model (Burri and Bleuler, 2013)

2.4.2 Dynamic Model of the Shoulder Complex

This section describes the dynamic model of the shoulder complex, for more detail cf. Ingram et al. (2012). The dynamic model of the shoulder complex is obtained using the Langrangian mechanics and the joint coordinates x_s. Each bone has a mass M_i and an inertia I_i (i = c, s, h) attached to the bone's center of gravity. The dynamic equation is given as:

$$M(x_s)\ddot{x}_s + h(x_s, \dot{x}_s) = f_{ext} \tag{2.4}$$

where $M(x_s)$ is the dynamic inertia matrix and $h(x_s, \dot{x}_s)$ is a vector containing the internal dynamics. The vector f_{ext} is the generalized external force.

The model includes 16 muscles which are divided into 28 segments. The segments are chosen according to anatomical criteria. The generalized external forces due to the muscles are calculated as follows:

$$f_{ext}^{msc} = \sum p_m \times f_m = P\,F \tag{2.5}$$

where P is the 9×28 moment arm matrix and F is the muscle force for each segment. The matrix P has one column for each muscle segment, and there are 9 rows because for each reference frame (clavicle, scapula and thorax) the moment arms are given. The dynamic model of the shoulder complex is given by the differential algebraic equations:

$$M(x_s)\ddot{x}_s = PF - h(x_s, \dot{x}_s) \tag{2.6}$$

2.5 Muscle Force Estimation

When estimating muscle forces in a biomechanical model a redundancy problem occurs. The redundancy problem is due to an over constraint set of equations of motion: The three equations for the moment equilibrium have as many unknowns as there are muscle forces, leading to an infinite number of solutions for this set of equations. With the help of an optimisation process and a suitable optimisation criteria a solution can be found.

2.5.1 Null-space Optimization

An optimization in mathematics is a process to find the most suitable solution out of all the possible solutions according to a given criteria. For the shoulder model in this project the criteria is:

Execute a given movement using minimal muscle stresses.

This criteria gives the additional equation necessary to solve the redundancy problem. So the optimal solution within the null-space can be found. The null-space describes the solution area of the given problem, meaning all the possible solutions.

2.5.2 Application for Shoulder Model

Considering a joint motion which is defined by $x_s(t)$, $\dot{x}_s(t)$ and $\ddot{x}_s(t)$, the generalized muscle forces can be defined by inverse dynamics as follows:

$$f_{ext}^{msc} = P\,F = M(x_s)\ddot{x}_s + h(x_s, \dot{x}_s) \tag{2.7}$$

The muscle force has to be positive and a maximum strength constraint is defined:

$$0 \leq F \leq F^{MAX} \tag{2.8}$$

To find a solution, the problem is defined as an optimization problem as in Equation 2.9. Where $g(F)$ is the cost function defined as the mean square of the muscle stresses (cf. 2.10).

$$\begin{aligned} min\ g(F) \\ s.t.\ 0 \leq F \leq F^{MAX} \\ f_{ext}^{msc} = P\,F \end{aligned} \tag{2.9}$$

$$g(F) = \sum_{i=1}^{n} \frac{(F_i/A_i)^2}{n} \tag{2.10}$$

In the cost function n is equal to the number of muscle forces that are to be computed and A is the physiological cross sectional area. For more detail refer to Ingram et al. (2012).

2.6 Musculoskeletal Joint Model in Matlab

The shoulder model was built using an existing approach (Ingram et al., 2012). The model consists of a preprocessor, that generates geometry and movement data, and a solver which runs the optimization process to compute muscle and joint reaction forces.

2.6.1 Bones

The anatomical data to describe the bones in the numerical model come from a reconstruction of MRI images in Amira. The MRI images were taken from a young and healthy individual. The definition of the bony landmarks and standardized definition of joint motion and local coordinate systems is taken from (Wu et al., 2005).

2.6.2 Muscles

In the existing numeric model the muscles are modelled as cables. As mentioned earlier, there are 16 muscles in the shoulder complex. These muscles are separated into 28 segments, chosen according to anatomical and topographical criteria. For example the deltoid muscle is split up in 3 segments according to their different origin locations.
In the currently used Matlab program one cable per segment is computed. To define one cable, an origin and an insertion point has to be defined. Furthermore, the reference frames of those points have to be specified. For some muscle segments it is necessary to define supplementary points called Via points. The cable passes through these points in order to have the correct lever arm. If necessary two Via points can be defined, one close to the insertion (Via A point) and one close to the origin (Via B point).

To further improve the anatomical representation of a muscle, the cable is guided along a wrapping object. The wrapping objects are different kinds of cylinders. Three types of wrapping object exist and are represented in the Table 2.5. For some segments no object is necessary. For each type of wrapping object, its center, its reference frame, its diameter and its z-axis direction has to be specified.

Wrapping Objects		
1 cylinder: '*single*'	2 cylinders '*double*'	Cylinder with demi sphere '*stub*'
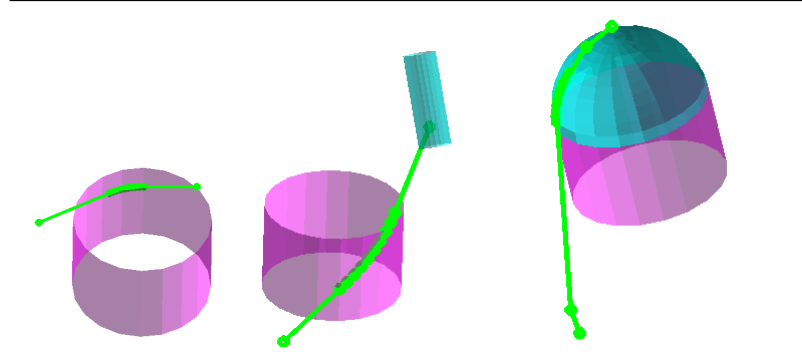
Table 2.5: Wrapping objects

The schematic in Figure 2.11 illustrates the path a cable has to follow.
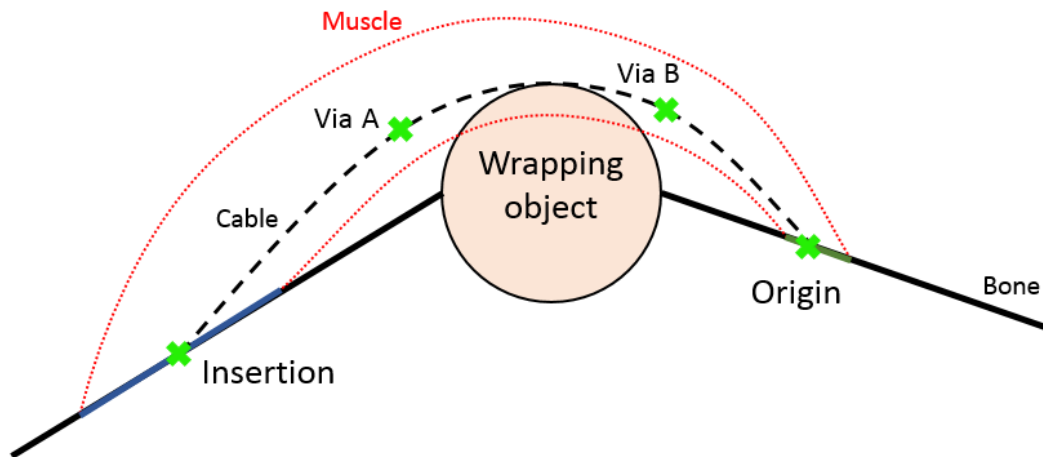
Figure 2.11: Illustration of cable path

2.7   Geometry

2.7.1   Straight Line

Two points are necessary to define a straight line. Assuming the line passes through the point A and B, and the corresponding vectors are:

$$\vec{a} = \begin{pmatrix} a_1 \\ a_2 \\ a_3 \end{pmatrix}, \quad \vec{b} = \begin{pmatrix} b_1 \\ b_2 \\ b_3 \end{pmatrix} \tag{2.11}$$

The parametrised line that passes through these two points is defined as:

$$r(t) = \vec{a} + t(\vec{b} - \vec{a}) \tag{2.12}$$

2.7.2   Spline Interpolation

The following section contains an introduction to spline interpolations, for more detail refer to Barbic (2011): A spline is a piecewise polynomial, where many low degree polynomials are used to interpolate the control points. Cubic splines use cubic polynomials to interpolate. They are the lowest order polynomials that interpolate 2 points and allow the gradient at each point to be defined (C^1 continuity is possible).

There are different types of splines. Here the Catmull-Rom spline, a special case of the cubic Hermite spline and is explained first. A cubic Hermite spline is a spline where each segment between two control points is a third-degree polynomial specified in 3D by the position and tangent vectors at the end points of the interval $[0, 1]$ (cf. Figure 2.12).

Figure 2.12: Hermite spline specification (Barbic, 2011)

Four constraints can be defined, the position and the tangent vectors of the two end points:

$$\begin{aligned}
p(0) &= p_1 = (x_1, y_1, z_1) \\
p(1) &= p_2 = (x_2, y_2, z_2) \\
p'(0) &= \bar{p}_1 = (\bar{x}_1, \bar{y}_1, \bar{z}_1) \\
p'(1) &= \bar{p}_2 = (\bar{x}_2, \bar{y}_2, \bar{z}_2)
\end{aligned} \tag{2.13}$$

The cubic form $p(u) = au^3 + bu^2 + cu + d$, is assumed which gives 4 unknowns a, b, c, d and leads to a linear system with 12 equations and 12 unknowns. After solving, the following form is obtained:

$$\begin{bmatrix} x(u) \, y(u) \, z(u) \end{bmatrix} = \begin{bmatrix} u^3 \, u^2 \, u \, 1 \end{bmatrix} \begin{bmatrix} 2 & -2 & 1 & 1 \\ -3 & 3 & -2 & -1 \\ 0 & 0 & 1 & 0 \\ 1 & 0 & 0 & 0 \end{bmatrix} \begin{bmatrix} x_1 & y_1 & z_1 \\ x_2 & y_2 & z_2 \\ \bar{x}_1 & \bar{y}_1 & \bar{z}_1 \\ \bar{x}_2 & \bar{y}_2 & \bar{z}_2 \end{bmatrix} \tag{2.14}$$

where (x, y, z) is a point on the spline segment, the parameter u varies between 0 and 1 and the last matrix is the control matrix containing the information about the control points. To have a multi segment Hermite spline the joining ends of two segments have to have maching positions and tangent vectors.

As mentioned, the Catmull-Rom spline is a special case of the Hermite splines. For the Catmull-Rom spline the tangent at the control point p_i is set to $s * (p_{i+1} - p_{i-1})$, where s is the tension parameter. This parameter determines the magnitude of the tangent vector at p_i. The two end points are used as extra control points at both ends of the spline to define the tangents there. So the spline segment between the control points p_i and p_{i+1} is completely defined by p_{i-1}, p_i, p_{i+1} and p_{i+2}.

The parametrized equation for a Catmull-Rom spline segment is in Equation 2.15. The parameter s is typically set to 0.5. The matrix depending on the parameter s is called basis and the matrix with the four points is called control matrix.

$$
[x(u)\ y(u)\ z(u)] = [u^3\ u^2\ u\ 1]
\begin{bmatrix}
-s & 2-s & s-2 & s \\
2s & s-3 & 3-2s & -s \\
-s & 0 & s & 0 \\
0 & 1 & 0 & 0
\end{bmatrix}
\begin{bmatrix}
x_1 & y_1 & z_1 \\
x_2 & y_2 & z_2 \\
x_3 & y_3 & z_3 \\
x_4 & y_4 & z_4
\end{bmatrix}
\tag{2.15}
$$

Using this type of spline, a spline made up of two segments can be formed with only three control points, where the first and the last point are used twice. An example can be seen in Figure 2.13. The first segment goes from p_i to p_{i+1}. To compute this segment the Equation 2.15 is used with the control matrix in Equation 2.16. The first control point p_i is used twice, to construct the first segment of the spline. For each segment the parameter u in Equation 2.15 varies from 0 to 1.(Barbic, 2011)

$$
\begin{bmatrix}
p_i(1) & p_i(2) & p_i(3) \\
p_i(1) & p_i(2) & p_i(3) \\
p_{i+1}(1) & p_{i+1}(2) & p_{i+1}(3) \\
p_{i+2}(1) & p_{i+2}(2) & p_{i+2}(3)
\end{bmatrix}
\tag{2.16}
$$

The arc length of a spline segment can be computed by summing up the discrete Δs (cf. Figure 2.13). The spline is in 3D hence the Δs is computed as in Equation 2.17.
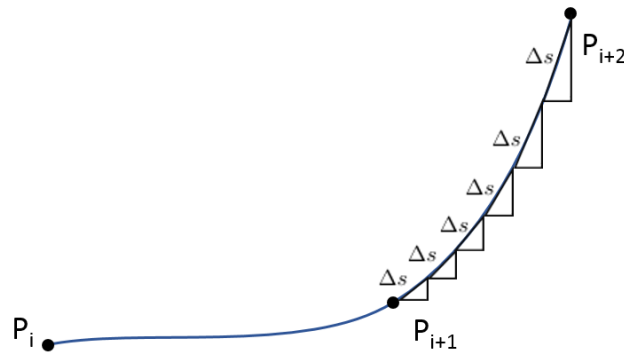
Figure 2.13: Illustration of arc length computation

$$
\Delta s = \sqrt{\Delta x^2 + \Delta y^2 + \Delta z^2}
\tag{2.17}
$$

The arc length of the first spline segment is equal to $\sum \Delta s_1$, and for the second spline segment $\sum \Delta s_1$.

Chapter 3

Methods

The Matlab model evaluates the muscle force per muscle segment necessary for a given movement. In the existing model there is one cable for each muscle segment. The goal is to implement the possibility to have multiple cables per segment. To achieve this goal, a new preprocessor for this model is implemented which allows to generate the data for the bones and configure the muscle cables before the solver computes the forces.

3.1 Muscle Modelling

A muscle inserts and originates from an area on a bone as schematized in Figure 3.1.
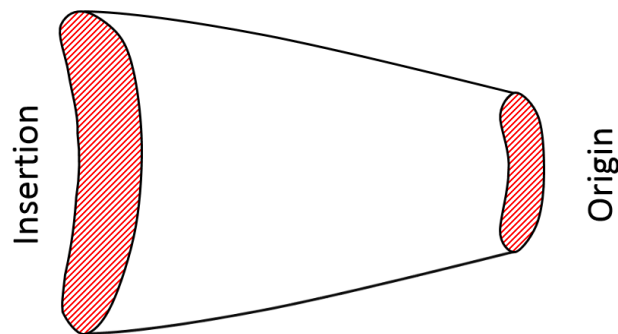
Figure 3.1: Schema of a muscle

In the current model these areas are approximated with one point. In order to have multiple cables per segment this area has to be approximated differently. Two new approaches to approximate the insertion and origin areas are implemented for this project. The first method consists in approximating the insertion and origin areas with a straight line as in Figure 3.2(a). For the second method, these areas are approximated with a Catmull-Rom spline (cf. Figure 3.2(a)).

(a) Line approximation   (b) Spline approximation
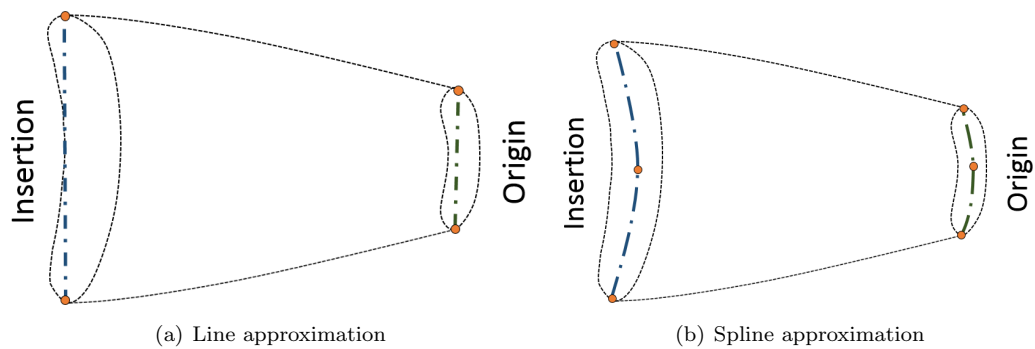
Figure 3.2: Illustration of two methods

The user can chose the number of cables for the muscle segments at each execution. The defined line, or spline, is split up to find the defined origin or insertion points necessary. For the Via points the same method is used.

As mentioned in the Section 2.7, two points are necessary to define a straight line and three points to define a Catmull-Rom spline. These points have to be defined on the insertion and origin areas on the bones on each muscle segment. The points necessary to set the Via points have to be defined as well. The points are placed visually on the anatomical reconstruction of MRI images of a young and healthy individual (cf. Section 2.2). An anatomical atlas was used to find the locations of the origin and insertion areas as well as the via points.

3.1.1 Straight Line Approximation

The two points on the anatomical reconstruction are chosen so that the line follows the bone as closely as possible. The two points are denoted A and B. The line has to be split up to find the necessary number of origin, insertion and via points to define each cable.

The muscle is considered as a volume, if there is one cable it passes through the middle. If there are two cables the volume of the muscle is separated into two equal parts and the cables pass through the middle of each section. The same is done for three cables and so forth, as illustrated in the Figure 4.11.

(a) One cable

(b) Two cables

(c) Three cables
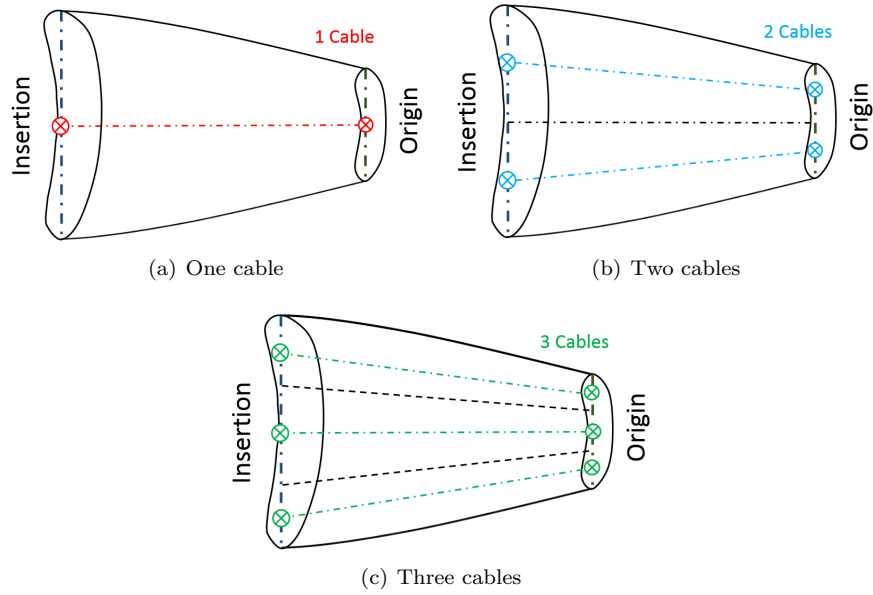
Figure 3.3: The cables distributed on a straight line

Looking at Figure 4.11, it is evident that if there is one cable it starts at $1/2$ of the line, if there are two cables they start at $1/4$ and $3/4$ of the line. The Figure 3.4 shows the two points A and B and their associated vectors $\vec{a}$ and $\vec{b}$. To find a point C on the line the Equation 3.1 is used.

(a) One point on a line

(b) Two points on a line
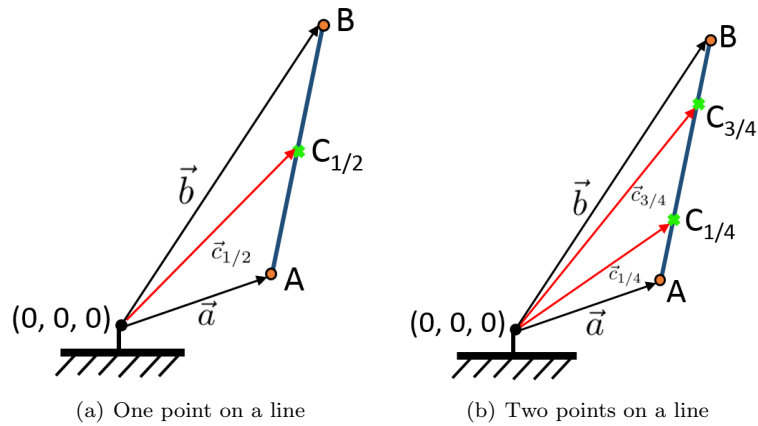
Figure 3.4: Method to split straight line

$$\vec{c} = \vec{a} + \lambda(\vec{b} - \vec{a}) \tag{3.1}$$

The parameter λ depends on the number of cables per muscle segment. The Table 3.1 shows the parameter depending on the number of cables. The parameter λ can be determined for any number of cables with the Equation 3.2.

$$\lambda = \frac{2 * Curr\_Muscle\_Cable - 1}{2 * Cable\_Array(Curr\_Muscle\_Segm)} \tag{3.2}$$

# cables	first cable	2nd cable	3rd cable	4rd cable	5th cable
1	$\lambda = 1/2$				
2	$\lambda = 1/4$	$\lambda = 3/4$			
3	$\lambda = 1/6$	$\lambda = 3/6$	$\lambda = 5/6$		
4	$\lambda = 1/8$	$\lambda = 3/8$	$\lambda = 5/8$	$\lambda = 7/8$	
5	$\lambda = 1/10$	$\lambda = 3/10$	$\lambda = 5/10$	$\lambda = 7/10$	$\lambda = 9/10$

Table 3.1: Row structure for the cable information cell array

3.1.2 Catmull-Rom Spline Approximation

When using a spline to approximate the origin and insertion areas the distribution of the cables is done similarly to the line approximation. The muscle is again considered as a volume and is split up. The Figure 3.5 shows the distribution of the cables on a spline.

(a) One cables

(b) Two cables

(c) Three cables
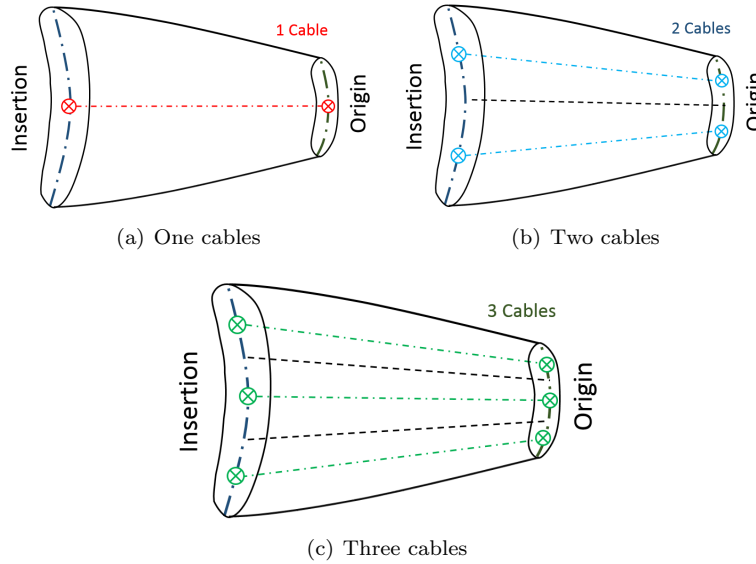
Figure 3.5: The cables distributed on a Spline

To find any points on a spline, its parametrized equation can be used. The parametrized equation is recalled here:

$$
\begin{bmatrix} x(u)\ y(u)\ z(u) \end{bmatrix} = \begin{bmatrix} u^3\ u^2\ u\ 1 \end{bmatrix} \begin{bmatrix} -s & 2-s & s-2 & s \\ 2s & s-3 & 3-2s & -s \\ -s & 0 & s & 0 \\ 0 & 1 & 0 & 0 \end{bmatrix} \begin{bmatrix} x_1 & y_1 & z_1 \\ x_2 & y_2 & z_2 \\ x_3 & y_3 & z_3 \\ x_4 & y_4 & z_4 \end{bmatrix} \tag{3.3}
$$

Each segment of the spline is defined by this parametrized equation and any point on the spline segment can be found by choosing the parameter u between 0 and 1. To split up the spline as in Figure 3.5 the arc length of the spline can be used. The total arc length of a spline, made up of two segments, is equal to the sum of the arc length of each segment:

$$
total\_arc\_length = \sum \Delta s_1 + \sum \Delta s_2 \tag{3.4}
$$

The computations of the arc length of one segment $\sum \Delta s$ is described in Section 2.7. A spline with two segments is illustrated in Figure 3.6.
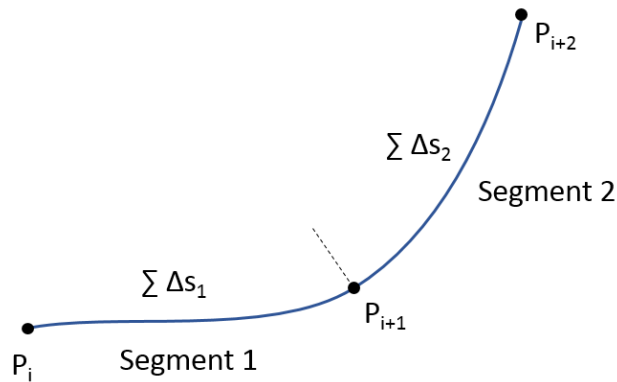
Figure 3.6: Arc length for a spline with two segments

As mentioned, the parameter u has to be determined to find a point on the spline segment. Since there are two spline segments there is a separate parameter for each segment, u_1 and u_2. For each segment the parameter goes from 0 to 1, as illustrated in Figure 3.7
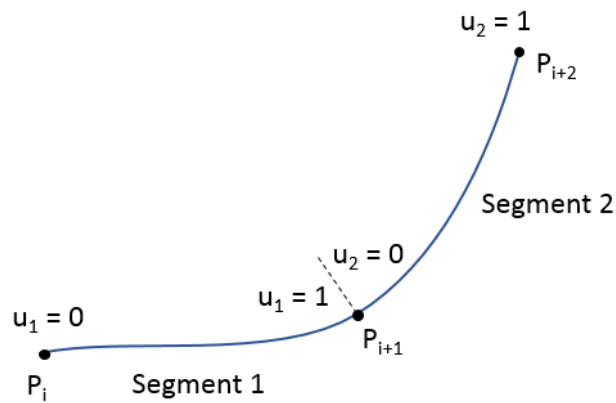
Figure 3.7: Parameter u for a spline with two segments

Once the total arc length of the spline is known, the parameter λ is used to split up the total arc length. Hence the target arc length for each desired point on the spline can be found:

$$target\_arc\_lenght = \lambda * total\_arc\_length \tag{3.5}$$

From the target arc length it can be determined on which spline segment the point is. In the case that the $target\_arc\_lenght$ is smaller than $\sum \Delta s_1$ the desired point C is on the first segment. To find the point C, the parameter u_1 has to be determined and entered in the the parametrized equation of the first spline segment. The parameter u_1 can be computed with the ratio of length in the first segment:

$$u_1 = \frac{target\_arc\_lenght}{\sum \Delta s_1} \tag{3.6}$$

If the $target\_arc\_lenght$ is bigger than the the length of the first segment, the point C is on the second segment of the spline. Hence the parameter u_2 has to be computed and entered in the parametrized equation of the second segment. The parameter u_2 is determined as follows:

$$u_2 = \frac{target\_arc\_length - \sum \Delta s_1}{\sum \Delta s_2} \tag{3.7}$$

3.2   Preprocessor Program Structure

The structure of the new preprocessor can be seen in Figure 3.8.
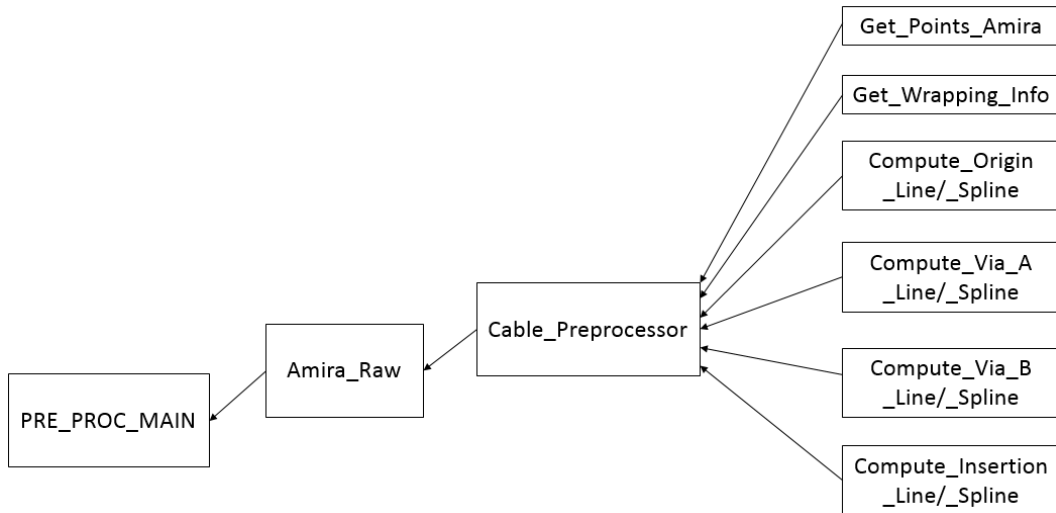
Figure 3.8: Flow chart for the preprocessor

The $PRE\_PROC\_MAIN.m$ file is the main file of the preprocessor, it controls the configuration of the bone and muscle structure and plots the chosen cable in the visualisation. The $Amira\_Raw.m$ file's output is the muscle data needed for the chosen cable. The computation of the muscle data for all cables is coordinated by the file $Cable\_Preprocessor.m$. The cable preprocessor calls all functions necessary to compute the origin, insertion, Via point and wrapping data necessary for each cable. Before executing the code, the user can choose how many cables should be computed per muscle segment. This is done by changing the values in the array $Cable\_Array$. The array's size is 28×1 and each row of the array corresponds to the number of cables in a muscle segment. Furthermore, the user chooses which cable of which segment should be drawn in the visualisation.

3.3   Data Structure

The data transfer from one function to the other is done via cell arrays. For one cable 13 parameters are necessary. Therefore, all cell arrays dealing with the cable data have 13 rows structured as in Table 3.2.

Parameters for one muscle cable

Row 1:	Pv :	Muscle Origin
Row 2:	Pref :	Origin Reference frame
Row 3:	Sv :	Muscle Insertion
Row 4:	Sref :	Insertion Reference frame
Row 5:	Ov :	Wrapping Object Center
Row 6:	Oref :	Wrapping Object Reference frame
Row 7:	Otype :	Wrapping Object type
Row 8:	Ozaxis :	Wrapping Object z axis direction
Row 9:	R :	Wrapping Object Diameter
Row 10:	Vav :	Via Point A (Near Insertion)
Row 11:	Varef :	Via Point A Reference System
Row 12:	Vbv :	Via Point B (Near Origin)
Row 13:	Vbref :	Via Point B Reference System

Table 3.2: Row structure for the cable data cell array

In the *get_Points_Amira* function the points from Amira are saved in cell arrays. The cell arrays have 28 columns, one for each muscle segment. There is one cell array for the insertion points, the origin points and the Via point.

The *get_Wrapping_Info.m* function fills a cell array (size 13×28) with the wrapping information and the different reference frames for each segment. The cell array *Cable_Data* is the one that saves all the information for all cables. Its size depends on the total number of cables. The total number of cables is the sum of all the elements in the *Cable_Array*. Hence the size of the *Cable_Data* cell array is $13 \times total\ number\ of\ cables$.

3.4   Numerical Studies

The new preprocessor has to be integrated in the existing solver in order that the muscle forces per cable can be computed. To get the muscle force per segment, the forces of all cables of that segment are summed up. The movement that is simulated for the first tests is the abduction of the arm up to 120°. The force can be plotted in function of the movement for each segment. The goal is to determine how many cables per segment are necessary to get consistent results in the muscle force.

First the muscle force necessary for the abduction, when the muscle is modelled as one cable, is computed. Then the number of cables per segment is increased and the computation is repeated. The solver computes the force for each cable. To get a force for one muscle segment the forces per cable have to be added up. For each of the 28 muscle segments a graph can be plotted. Each graph will show the evolution of the force in a given muscle segment in function of the movement. There is one curve per number of cables in each graph. The curves for the trapzius C7, deltoid acromial and supraspinatus will be analysed in detail. These three muscle segments were chosen because they are important for the abduction movement.

To compare the results for the different number of cables, two indexes are used. The first is the so called Smoothness Index. To determine the smoothness, the jumps of the curve have to be evaluated. The jumps in each curve are counted and their height is measured. To count the number of jumps in a curve, the second order derivative is used. The second order derivative describes the curvature of a function, and per jump in the original curve there is a peak in the second order derivative. The threshold for a change in the curve to be categorised as a jump is defined at 5 Newton. The Smoothness Index is defined as the number of peaks $\sum j$ multiplied with their average height H.

$$Smoothness\_Index = mean(H) * \sum j \tag{3.8}$$

This gives an index for every number of cables per muscle segment. It shows whether the curves get smoother after a certain number of cables.

The second index helps to determine how many cables are necessary to get consistent results of the muscle forces. The index used is the root mean square (RMS) error. The RMS error between two consecutive number of cables is computed:

$$RMS\,error = \sqrt{(mean(data - estimate)^2)} \tag{3.9}$$

With this index the difference between two consecutive curves can be evaluated. I.e. if the curve for 3 and 4 cables are compared, the force curve for 4 cables is taken as the *data* and the force curve for 3 cables is the *estimate*. If the RMS error gets smaller this means that the difference between the computed force per amount of cable decreases. Both indexes are plotted in graphs in function of the number of cables in a segment. The evolution of these indexes is presented and then discussed in the following chapters of the report.

Chapter 4

Results

The first step is to compare the two methods to generate the muscle data. The comparison between the line and the spline approximation is done visually. The Figure 4.1 shows the posterior part of the deltoid muscle once with the Line approximation (Figure 4.1(a)) and once with the spline approximation (Figure 4.1(b)). The Figure 4.1(b) shows that the spline follows the form of the bone more closely, which was to expect. All further simulations will be done using the spline approximation.

(a) Line approximation   (b) Spline approximation
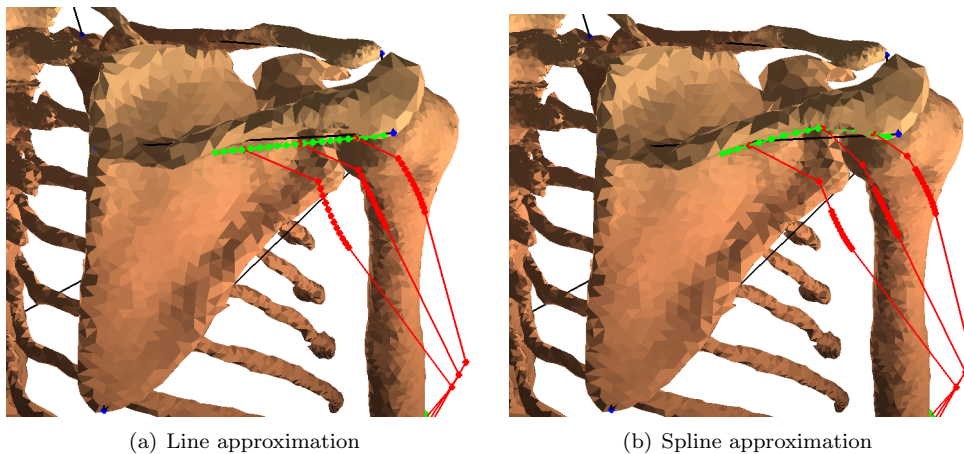
Figure 4.1: Comparison between two approximation methods

In the following paragraphs the force curves for the muscle segments trapzius C7, deltoid acromial and supraspinatus are presented. The two indexes are computed and plotted for these three segments. The force curves for the remaining muscle segments can be found in Appendix B.

The result for the trapezius C7 muscle segments, which originates from the 7th cervical vertebra, can be seen in Figure 4.2.
Per amount of cables there is one curve for the force evolution. The black dash-dot curve represents the evolution of the force for one cable. The blue line represents the force for two cables. For the trapzius C7 segment, modelled with two cables, the force increases up to about 80° of abduction. Afterwards, jumps appear in the force curve. The green line in the graph shows the force using three cables, here the number of jumps decreases. Even if the number of cables is increased, there are still jumps in the curves but their height decreases. To quantify the observed jumps the Smoothness Index is computed. The second order derivative can be seen in the Figures 4.3 for the trapzius C7 segment for one to six cables.
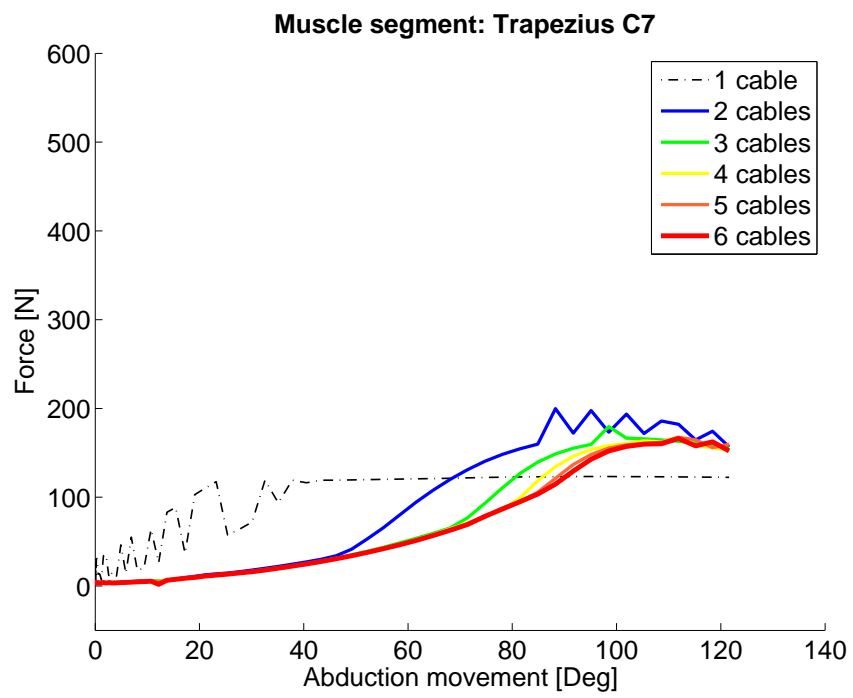
Figure 4.2: Trapzius C7
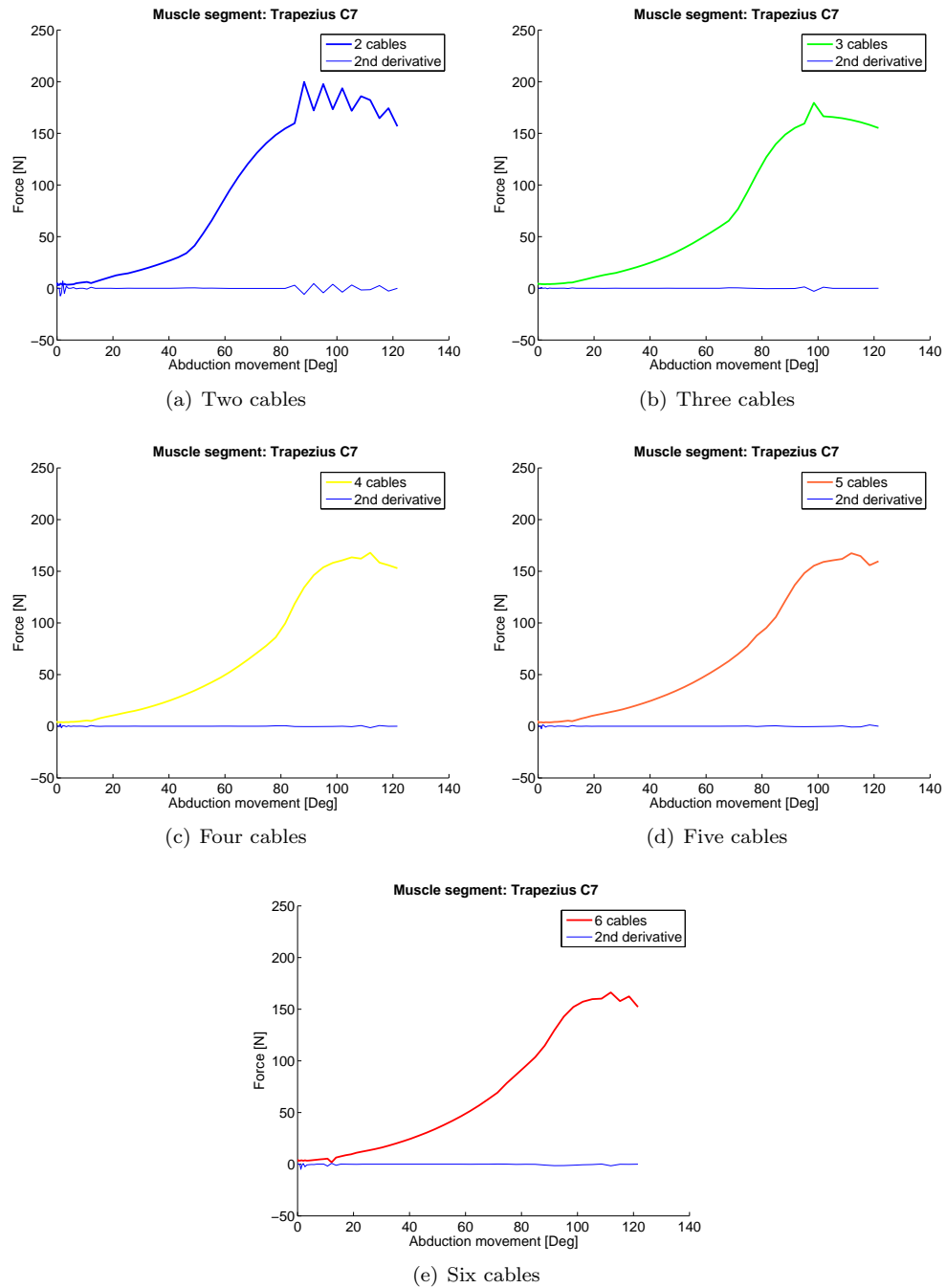
Figure 4.3: The second order derivative for the trapezius C7 muscle segment

For the trapezius C7 segment the Smoothness Index is calculated for one to 11 segments and is plotted against the number of cables. The plot can be seen in Figure 4.4. The index decreases up to 3 cables and then stabilizes, after 7 cables it starts to increase again.

Muscle segment: Trapzius C7
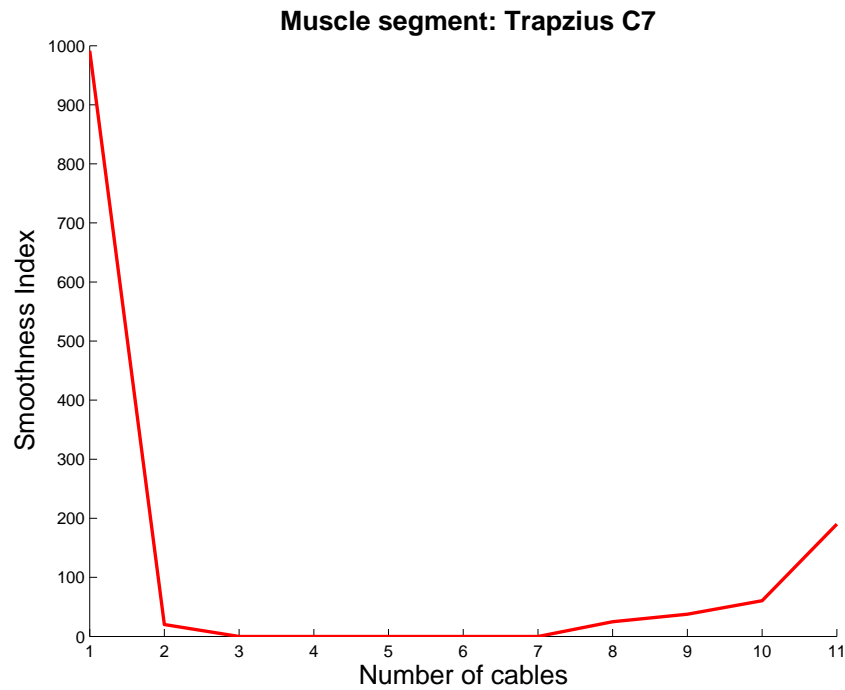
Figure 4.4: Smoothness Index for Trapzius C7

The RMS error is computed to see the difference between two consecutive number of cables. This has been done for the trapzius C7 segment and the plot for up to 11 cables can be seen in Figure 4.5.

Here the same observation as before can be made. For the trapezius C7 segment the RMS error decreases between 1 and 3 cables before it stabilizes.

Muscle segment: Trapezius C7

Figure 4.5: Trapzius C7
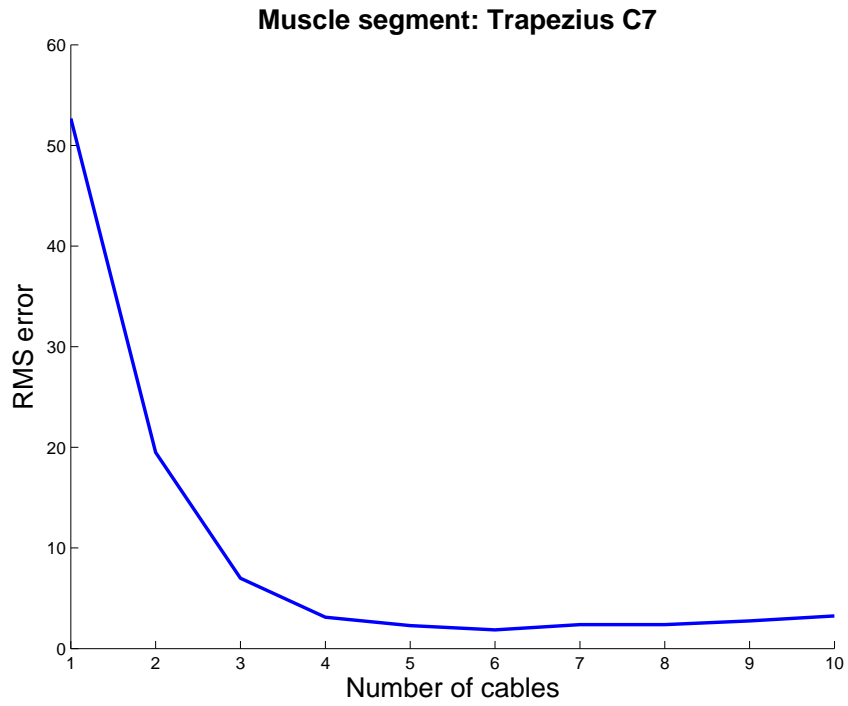
Muscle segment: Deltoid Acromial
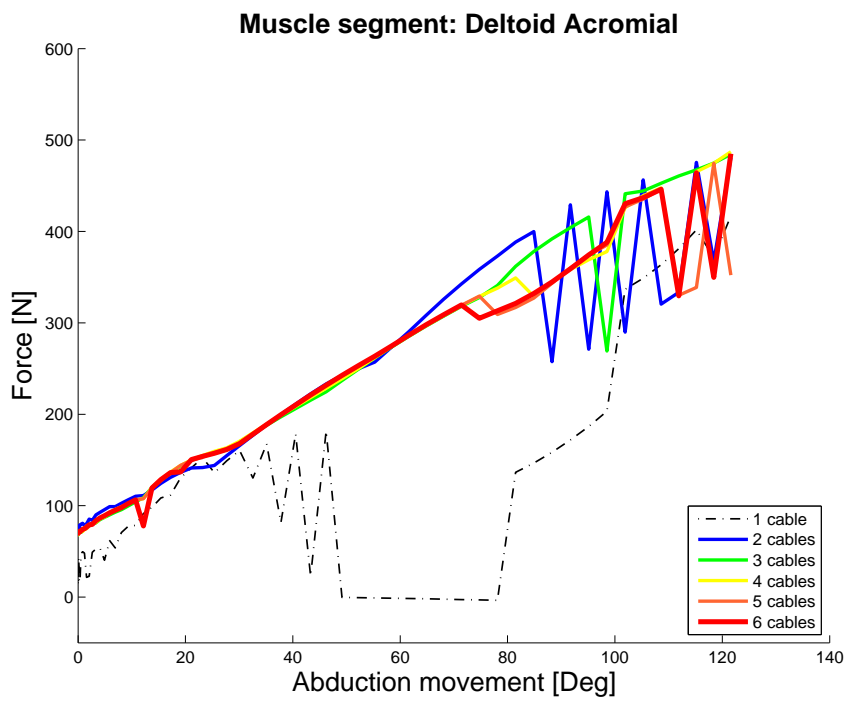
Figure 4.6: Deltoid acromial segment

(a) One cable

(b) Two cables

(c) Three cables

(d) Three cables

(e) Three cables
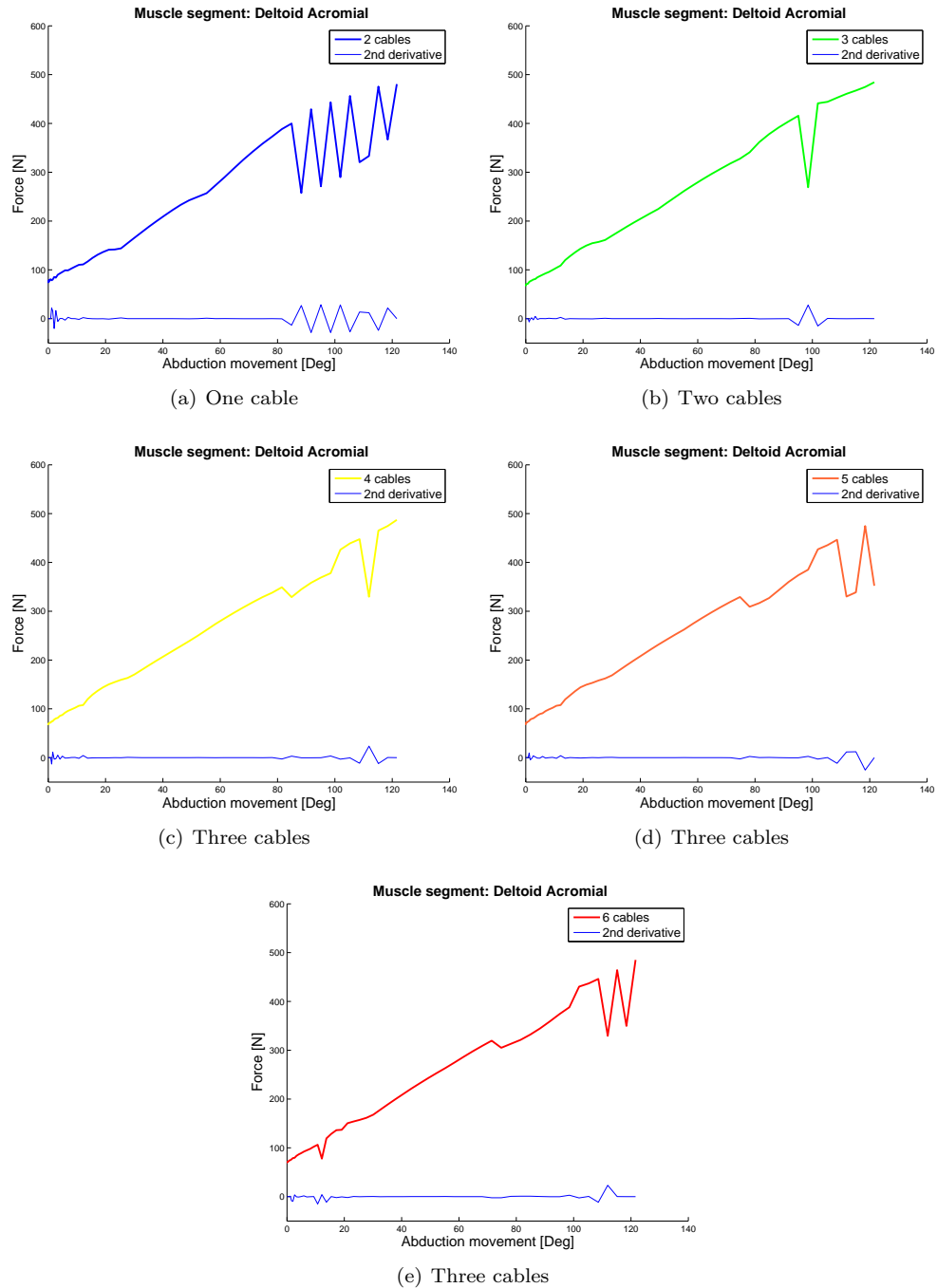
Figure 4.7: The second order derivative for the deltoid acromial muscle segment

The Figure 4.6 shows the force for the middle part of the deltoid muscle, originating from the acromial process. The force for all number of cables increases up to about 80° where jumps start to occur. The second order derivatives in Figure 4.7 correspond to this observation. The Smoothness Index in Figure 4.8 decreases from 1 to 3 cables and stabilizes up to 7 cables. With more then 7 cables the Smoothness Index increases again.
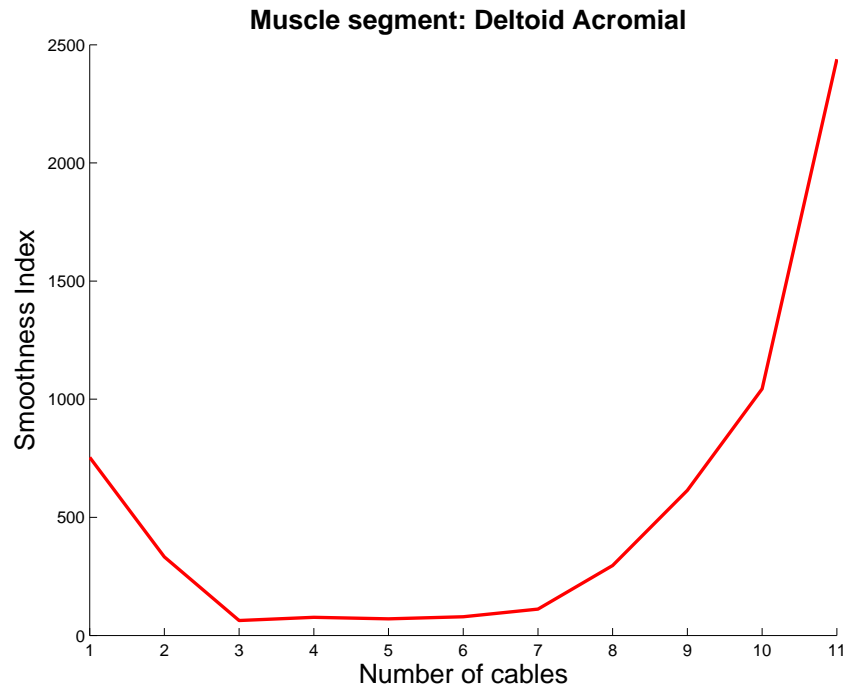
Figure 4.8: Smoothness Index for Trapzius C7

The RMS error for the deltoid acromial decreases up to 3 cables and then stabilizes as well. Again there is a slight increase after 7 cables.
The Figure 4.10 shows the force evolution for the supraspinatus segment.
The evolution of the Smoothness Index for the supraspinatus is similar to the previously discussed segments. It decreases up to 3 cables, stabilizes and increases again after 7 cables. The RMS error for the supraspinatus decreases up to 4 cables and then stabilizes.

Muscle segment: Deltoid Acromial

Figure 4.9: Trapzius C7
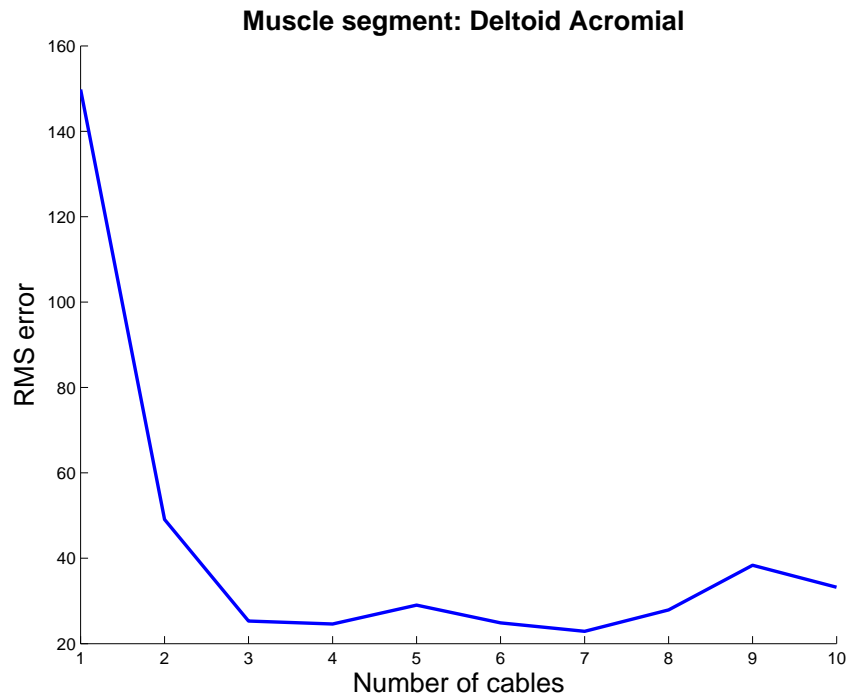
Muscle segment: Supraspinatus
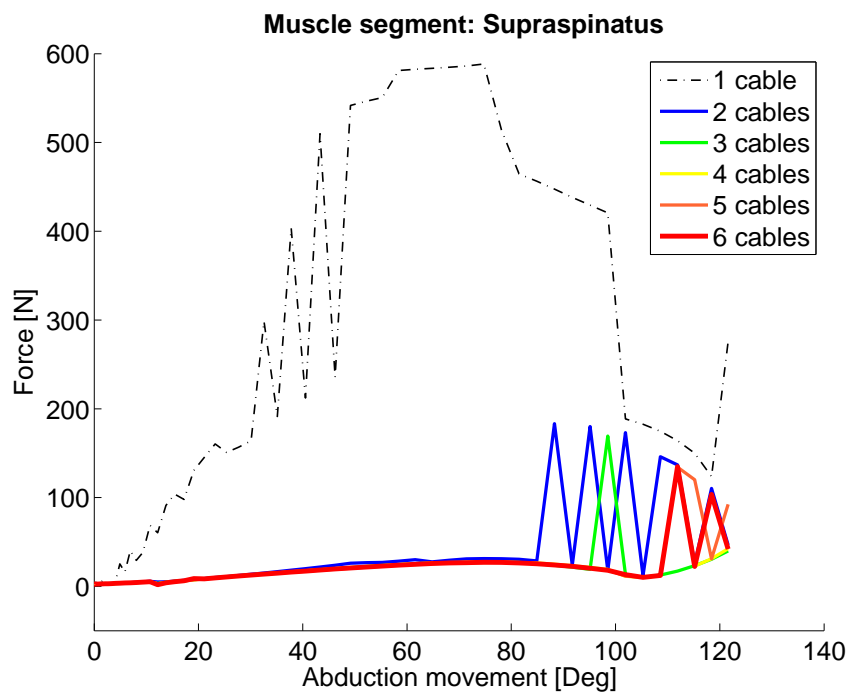
Figure 4.10: Supraspinatus segment

(a) One cable

(b) Two cables

(c) Three cables

(d) Three cables

(e) Three cables
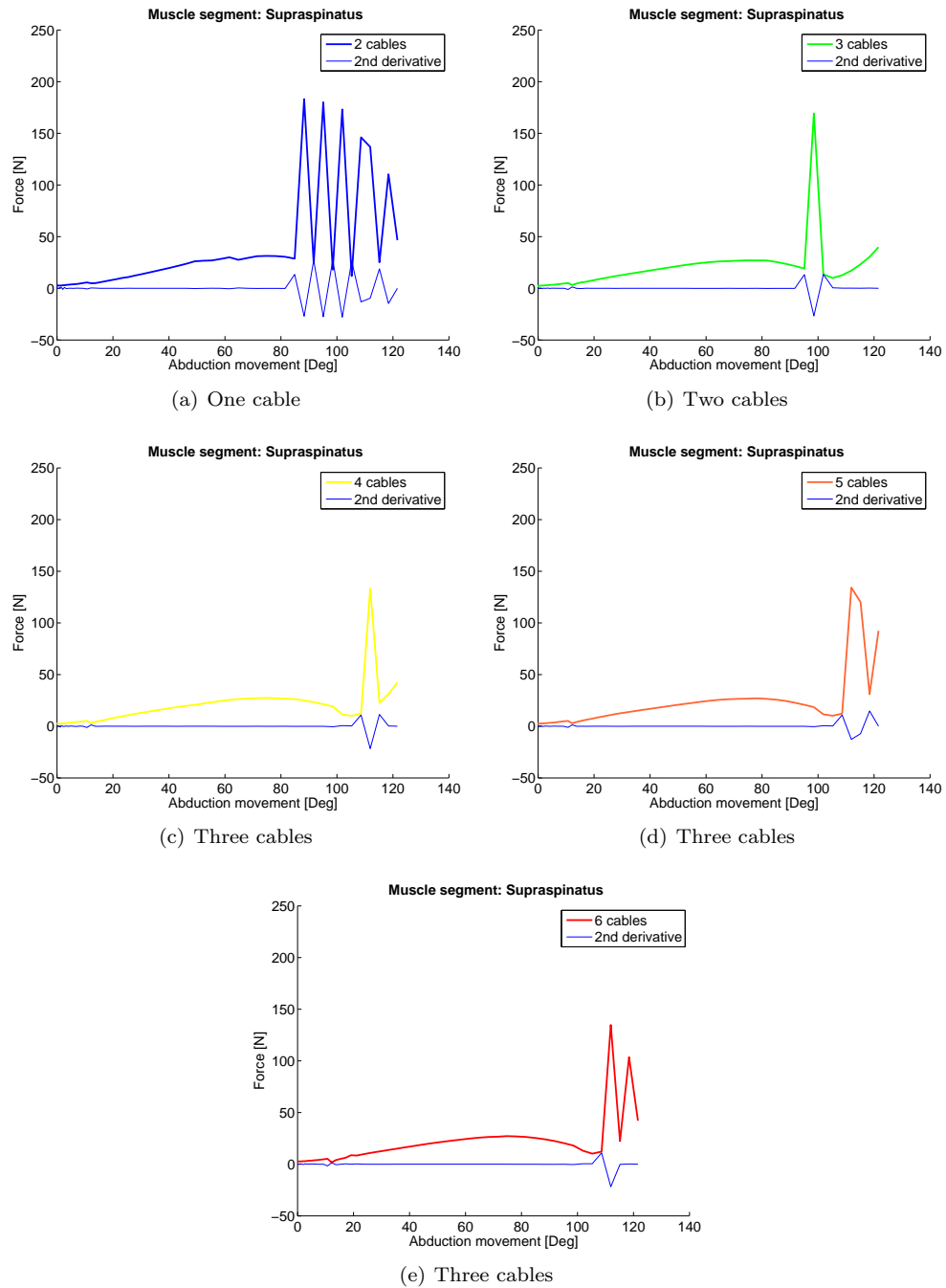
Figure 4.11: The second order derivative for the deltoid acromial muscle segment
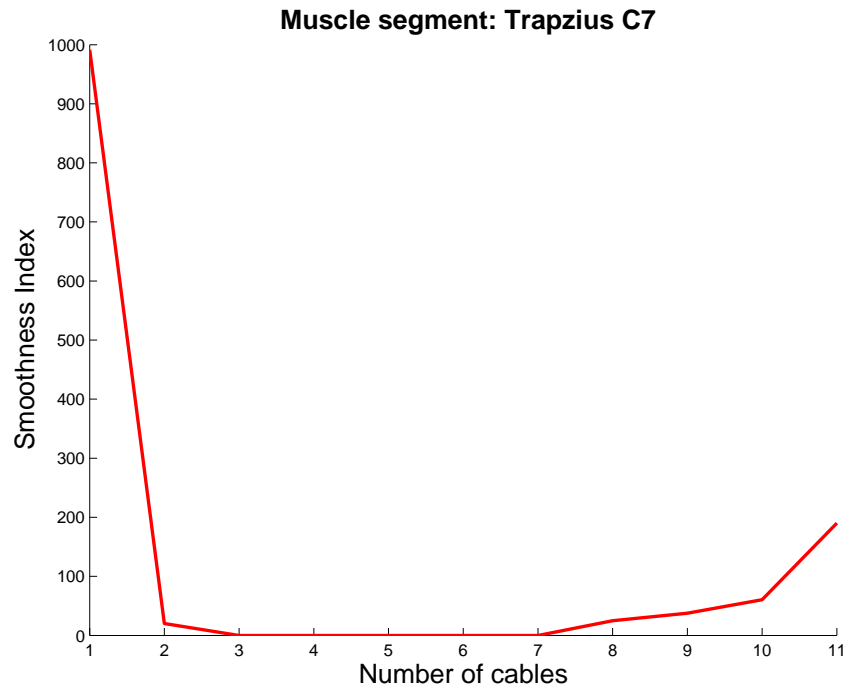
Figure 4.12: Smoothness Index for supraspinatus segment
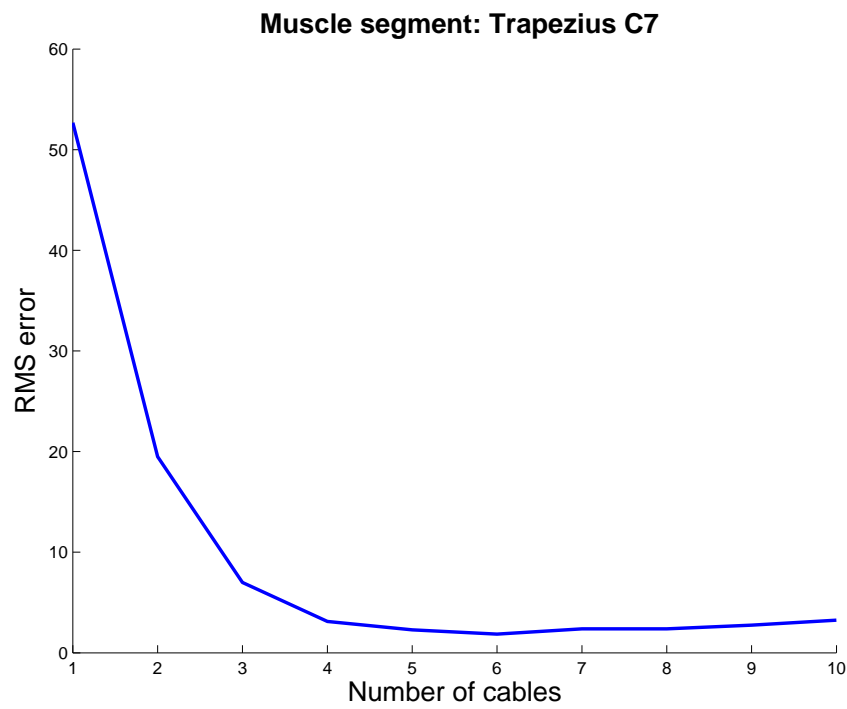
Figure 4.13: RMS error for the supraspinatus segment

Chapter 5

Discussion and Conclusion

The goal of the numerical study was to determine the minimal number of cables per muscle segment necessary to get consistent results for the muscle forces.

A strong point of the musculoskeletal joint model used for the numerical studies is the fact that the model simulates all the muscles in the shoulder complex. Furthermore, the model is dynamic and every movement of the shoulder can be simulated. An other advantage is that the model is programmed on Matlab, which can be used on any operating system.

However, the model has some limitations. The fact that the muscles were split up according to anatomical criteria can be seen as a limitation. The question is, whether this is the best method to separate the muscles into segments. To estimate the muscle forces in the model it would possibly be better to consider physiological criteria. Such as the innervation of the muscles or their function.

There are the limitations of a 1D representation of muscles in general. A muscle is a very complex 3D structure in the human body. If the muscle is modelled as one cable, meaning as 1D, the line of action of the muscle is not exact. Furthermore, the distribution of the fibres is neglected and the interaction between different muscles and underlying structures cannot be taken into consideration. The advantage of the 1D model is its simplicity. It is simple to implement and the computational effort is small.

For the numerical study conducted multiple cables per muscle segment were implemented and distributed on a spline. This could be seen as a 2D model of the muscle. Compared to the 1D model, the 2D representation of a muscle represents the complex structure of the muscle more realistically. The line of action of the muscle is improved and the notion of muscle fibres is taken into account. However, it is still an approximation compared to the 3D structure of the muscle.

The force estimation is computed using an optimisation algorithm. The criteria used is: *Execute a given movement with minimal muscle stresses*. This is a purely mechanical criteria, which represents an other limitation of the model. By taking a mechanical criteria the stabilizing functions of the muscles are not taken into consideration. With the current criteria only the muscle segments necessary for the movement are activated. However, there are muscle segments that are not directly implied in the movement but stabilize the shoulder during the execution of the movement. Instead of using the stress-based method to solve the redundancy, the electromyography(EMG)-based method could be used, for more detail refer to (Engelhardt et al., 2014).

As mentioned earlier, the 2D representation of the muscle is done either with a line or a spline method. The two methods to distribute several cables for one muscles segment were compared in Section 4. When approximating an area on the bone with a straight line, the problem is that the bone is not straight but has curves. For some origin and insertion areas the line approximation would be sufficient, i. e. the insertion of the deltoid on the humerus is on a straight line. However, the origin of the deltoid acromial is on the scapular spine which makes a curve. So if this insertion site is approximated with a line, the line does not follow the bone. With a spline approximation however, the spline can follow the curvature of the bone.

The question to answer with the numerical study is: *How many cables per muscle segment are necessary to get consistent results of the muscle force?*
The results for the three muscle segments trapzius C7, deltoid acromial and supraspinatus are presented in the previous chapter. The computations for one cable per segment yield inconsistent results. The problem is that the solver cannot find a solution within the optimization criteria if there is only one cable. This is due to the moment equilibrium at the sternoclavicular joint, which cannot be satisfied.
To quantify the observations in the force graphs, two indexes are used. The Smoothness Index and the RMS error. The Smoothness Index quantifies the jumps observed in the force curves. The jumps can be explained with the used optimisation criteria. The solver tries to satisfy the criteria at each movement step. The distribution of the force per muscle segment is decided at each step to fulfil the criteria. If from one step to the other another segment is closer to the optimal solution, there will be abrupt changes in the force which lead to jumps in the curves. The RMS error quantifies whether the force curves converge to one result when increasing the number of cables.
When evaluating the indexes for the trapezius C7, the deltoid acromial and the supraspinatus segment both the indexes decrease until the muscles are modelled with 3 to 4 cables. Then the indexes stabilize. For the Deloid Acromial the indexes increase again with more than 7 cables. For the Trapezius C7 and the Supraspinatus the Smoothness Index increases also with more than 7 cables but the RMS error stays stable.
The decreasing Smoothness Index indicates that both the number and height of the jumps decrease between 1 and 3 cables for all three segments. For more than 3 cables the index is stabilized which means that the number or the height of the jumps do not change any more. The decreasing RMS errors means that the difference between two consecutive cable numbers decreases. If the RMS erros stabilizes the muscle forces have converged to one result. These observations lead to the conclusion that 3 or more cables are necessary to get consistent results in the muscle forces.

However, the number of cables should not be increased to more than 7 cables because both indexes start to increase again after 7 cables. This means that there are either more jumps or higher jumps in the curves as well as a bigger difference between two consecutive cables. If the number of cables per segment is increased the computations get more complicated. Increasing the number of cables also increases the number of variables further in the already over-constraint set of equations (c.f. Section 2.5). The computation of the null-space requires a numerical matrix inversion which looses precision with increasing matrix sizes. Thus the quality of the solution will also decrease resulting in discontinuous force curves.

As the model is now, it is possible to estimate the muscle forces in the shoulder complex for multiple cables per muscle segment. The adapted model will help to further understand the complex kinematic system of the shoulder. The improved computation of muscle and joint reaction forces will also help to further understand muscle coordination and articular mechanics. It is however possible to continue working and improving the musculoskeletal joint model of the shoulder.

A possible next step is to test the model with an alternative optimisation criteria, as mentioned earlier. Furthermore, the results of the numerical studies can be compared to experimental data to validate the model. Another step is to further improve the modelling muscle structure. Now the muscles are modelled in 2D, the cables are distributed on a spline. One could try to model the muscles as close as possible to their 3D structure. Instead of approximating the areas on the bone with a spline or a line, it could be approximated by a finite number of points distributed on the area. For each cable a point among these points has to be chosen according to a given algorithm.

5.1   Acknowledgement

At this point I would like to thank my assistant Christoph Engelhardt for his help and support during this semester project. I would also like to thank David Ingram for his work on the model which made it possible for me to test the newly implemented methods.
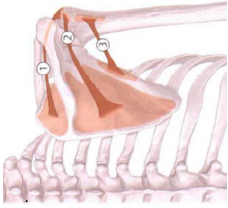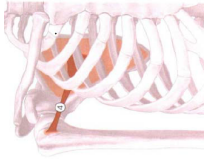
Bibliography
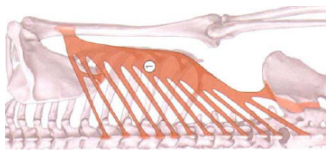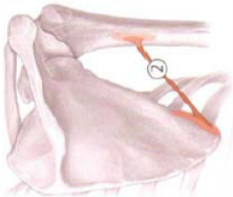
Amira online. May 2014. Amira homepage. `http://www.vsg3d.com/amira/overview`.

Barbic J., 2011. Script: CSCI 480 Computer Graphics. Georgia Institute of Technology (GT), Atlanta, Georgia.

Burri M. and Bleuler H., 2013. Lecture notes: Base de la robotique. Ecole polytechnique fédéral de Lausanne (EPFL), Lausanne.

Engelhardt C., Malfroy Camine V., Ingram D., Muellhaupt P., Farron A., Pioletti D. and Terrier A. 2014. Comparison of an emg-based and a stress-based method to predict shoulder muscle forces. Computer Methods in Biomechanics and Biomedical Engineering. URL `http://www.scopus.com/inward/record.url?eid=2-s2.0-84897353666&partnerID=40&md5=9e58b933723eed7bd9c30c04f3650047`.

Hansen J., 2010. Netter's Clinical Anatomy. Saunders Elsevier, Philadelphia. ISBN 978-1-4377-0272-9.

Ingram D., Muellhaupt P., Terrier A., Pralong E. and Farron A. 2012. Dynamical biomechanical model of the shoulder for muscle-force estimation. Proceedings of the IEEE RAS-EMBS International Conference on Biomedical Robotics and Biomechatronics. 407–412.

Pioletti D., 2013. Script: Biomechanics of the musculoskeletal system. Ecole polytechnique fédéral de Lausanne (EPFL), Lausanne.

Schuenke M., Schulte E. and Schumacher U., 2010. Atlas of Anatomy: General Anatomy and Musculoskeletal System. Georg Thieme Verlag, Stuttgart. ISBN 978-1-60406-292-2.

Terry G. and Chopp T. 2000. Functional anatomy of the shoulder. Journal of Athletic Training. 35(3), 248–255. URL `http://www.scopus.com/inward/record.url?eid=2-s2.0-0347561430&partnerID=40&md5=f16331318751657e1392b43c1927c84c`.

Wu G., Van Der Helm F., Veeger H., Makhsous M., Van Roy P., Anglin C., Nagels J., Karduna A., McQuade K., Wang X., Werner F. and Buchholz B. 2005. Isb recommendation on definitions of joint coordinate systems of various joints for the reporting of human joint motion - part ii: Shoulder, elbow, wrist and hand. Journal of Biomechanics. 38(5), 981–992. URL `http://www.scopus.com/inward/record.url?eid=2-s2.0-20144387878&partnerID=40&md5=0061c16426841273a89a29ca540b2283`.

Appendix A

Origin and Insertion for Shoulder Muscles

A.1   Muscles of the Shoulder Joint

Muscle	Image	Origin	Insertion	Main action
Supraspinatus		Supraspinous fossa of scapula	Superior facet on greater tubercle of humerus	Helps deltoid abduct arm at shoulder and acts with rotator cuff muscles
Infraspinatus		Infraspinous fossa of scapula	Middle facet on greater tubercle of humerus	Laterally rotates arm at shoulder; helps to hold head in glenoid cavity
Teres minor		Lateral border of scapula	Inferior facet on greater tubercle of humerus	Laterally rotates arm at shoulder; helps to hold head in glenoid cavity
Subscapularis		Subscapular fossa of scapula	Lesser tubercle of humerus	Medially rotates arm at shoulder and adducts it; helps to hold head in glenoid cavity

Muscle		Origin	Insertion	Action
Deltoid: Anterior part(1) Middle part (2) Posterior part (3)		Lateral third of clavicle, acromion and spine of scapula	Deltoid tuberosity of humerus	*Anterior part:* Flexes and medially rotates arm at shoulder *Middle part:* Abducts arm at shoulder *Posterior part:* Extends and laterally rotates arm at shoulder
Latissimus dorsi		Spinous processes of T7-T12, thoracolumbar fascia, iliac crest and inferior three or four ribs	Intertubecular groove of humerus	Extends, adducts and medially rotates humerus at shoulder
Teres major		Dorsal surface of inferior angle of scapula	Medial lip of intertubercular groove of humerus	adducts arms and medially rotates shoulder
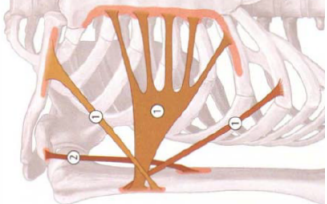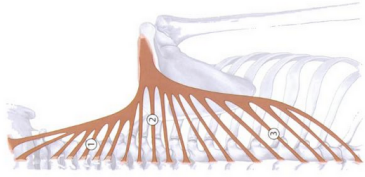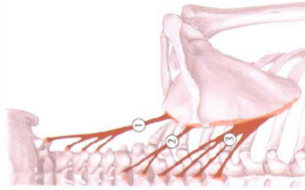
Pectoralis major		Medial half of clavicle sternum superior six costal cartilages; aponeurosis of external abdominal oblique	intertubercular groove of humerus	Flexes, adducts and medially rotates arm at shoulder
Coracobrachialis		Tip of coracoid process of scapula	Middle third of medial surface of humerus	Helps to flex and adduct arm at shoulder

Table A.1: Muscle of the shoulder joint; origin, insertion and function. Figures: (Schuenke et al., 2010) and text: (Hansen, 2010)

A.2   Muscles Migrated from the Trunk

Muscle	Image	Origin	Insertion	Main action
Trapezius		Medial third of superior nuchal line; external occipital protuberance, ligamentum nuchae and spinous processes of C7-T12	Lateral third of clavicle, acromion and spine of scapula	Elevates, retracts and rotates scapula; superior fibers elatvate, middle fibres retract and inferior fibres depress scapula
Levator scapulae (1)		Transverse process of C1-C4	Superior part of medial border of scapula	Elevates scapula and tilts its glenoid cavity inferiorly by rotation the scapula
Rhomboid minor(2)		Ligamentum nuchae and spinous processes of C7 and T1	Medial border of scapula above spine	Retracts scapula and rotates it to depress glenoid cavity; fixes scapula to throacic wall
Rhomboid major (3)		Spinous processes of T2-T5	Medial border of scapula below spine	Retracts scapula and rotates it to depress glenoid cavity; fixes scapula to throacic wall
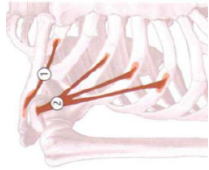
Subclavius (1)	Junction of first rib and costal cartilage	Inferior surface of clavicle	Depresses clavicle
Pectoralis minor (2)	Third to fifth rip	Coracoid process of scapula	Depresses scapula and stabilizes it
Serratus anterior	Upper eight ribs	Medial border of scapula	Rotates scapula upward, and pulls it anterior toward thoracic wall

Table A.2: Muscle migrated from the Trunk; origin, insertion and function. Figures: (Schuenke et al., 2010) and text: (Hansen, 2010)

Appendix B

Results: Force Graphs
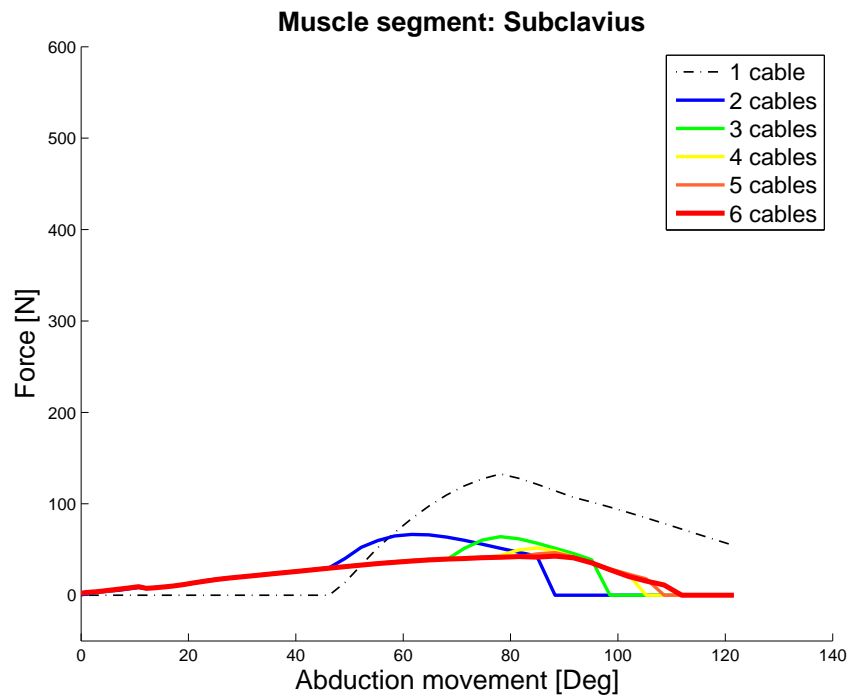
Figure B.1: Subclavius
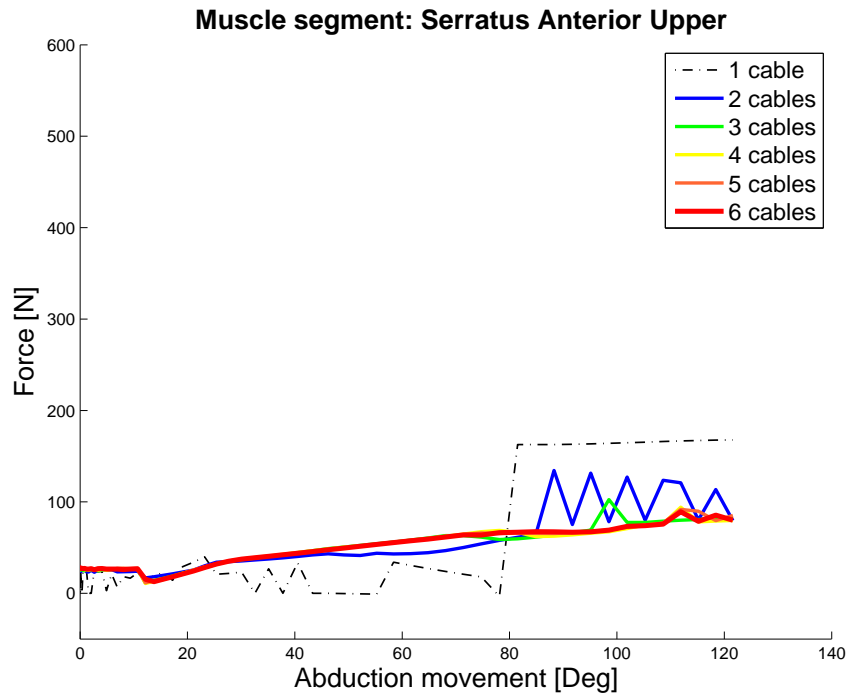
Figure B.2: Serratus Anterior Upper
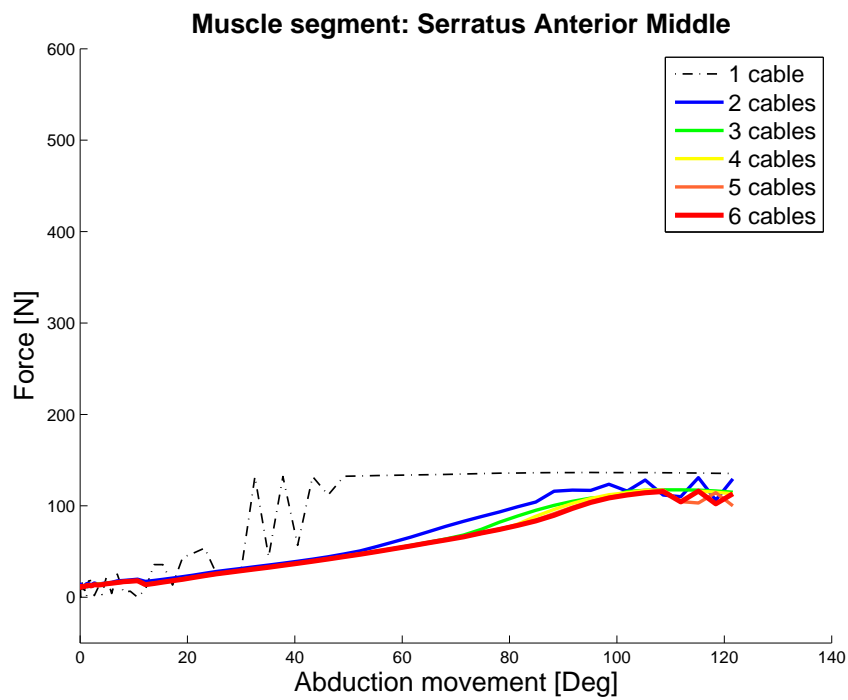
Figure B.3: Serratus Anterior Middle

Muscle segment: Serratus Anterior Lower
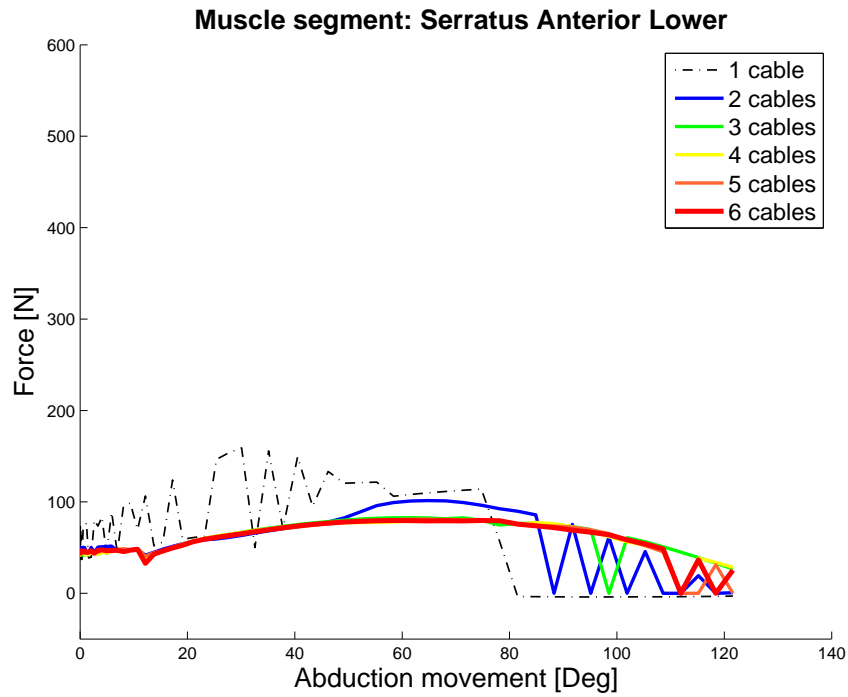
Figure B.4: Serratus Anterior Lower

Muscle segment: Trapezius C1 – C6
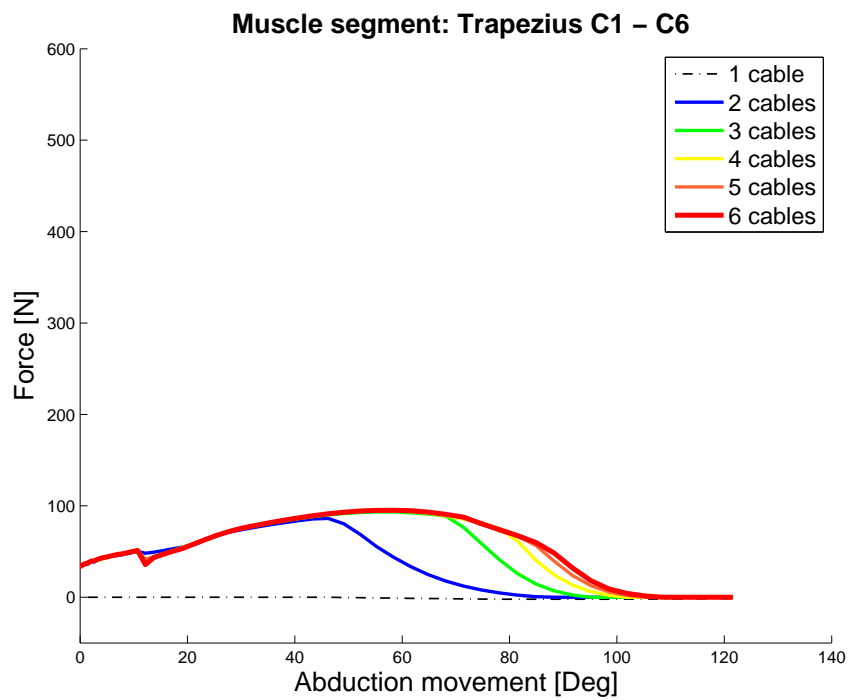
Figure B.5: Trapezius C1 - C6
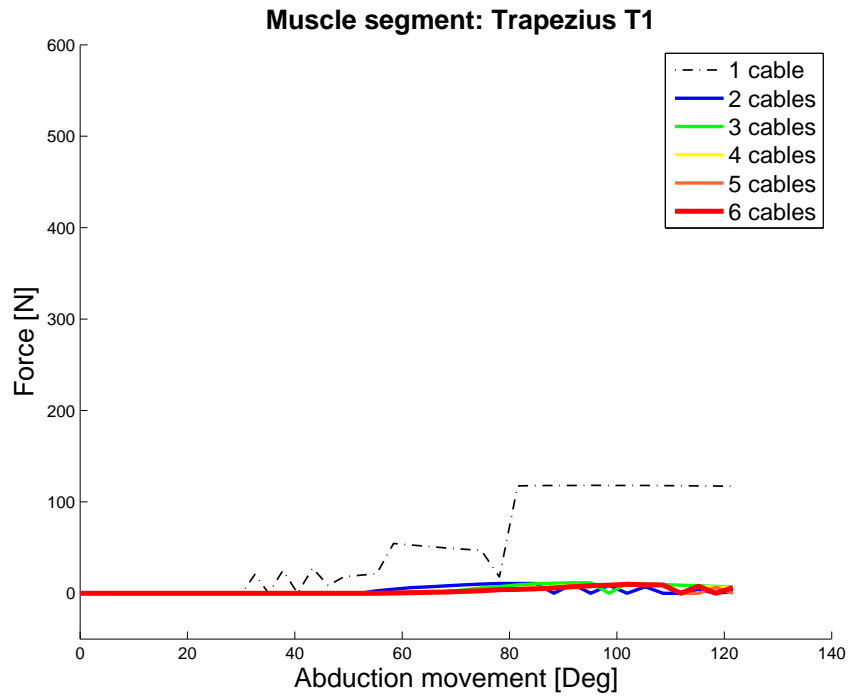
Figure B.6: Trapzius T1
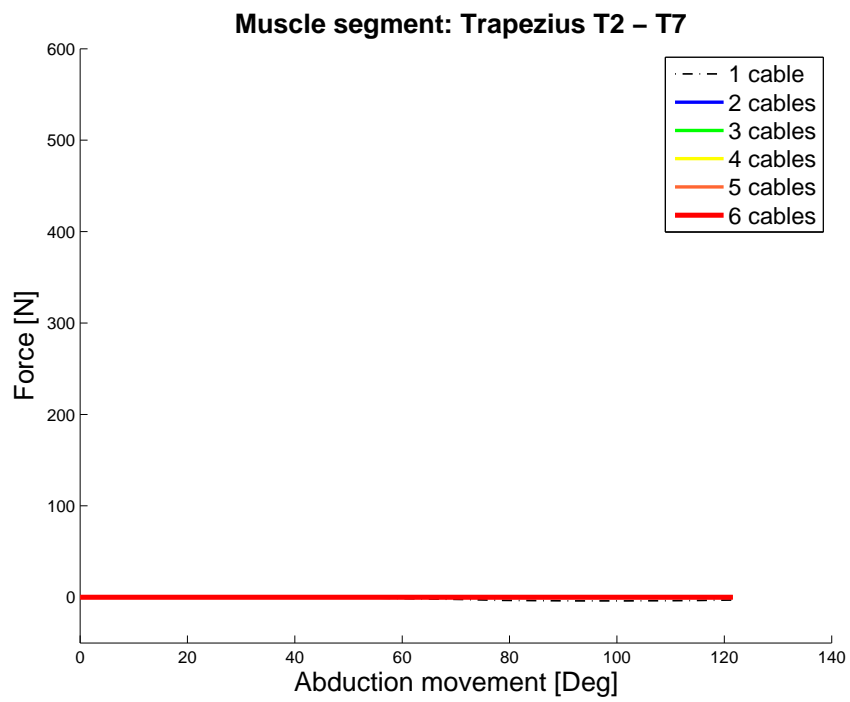
Figure B.7: Trapzius T2-T7
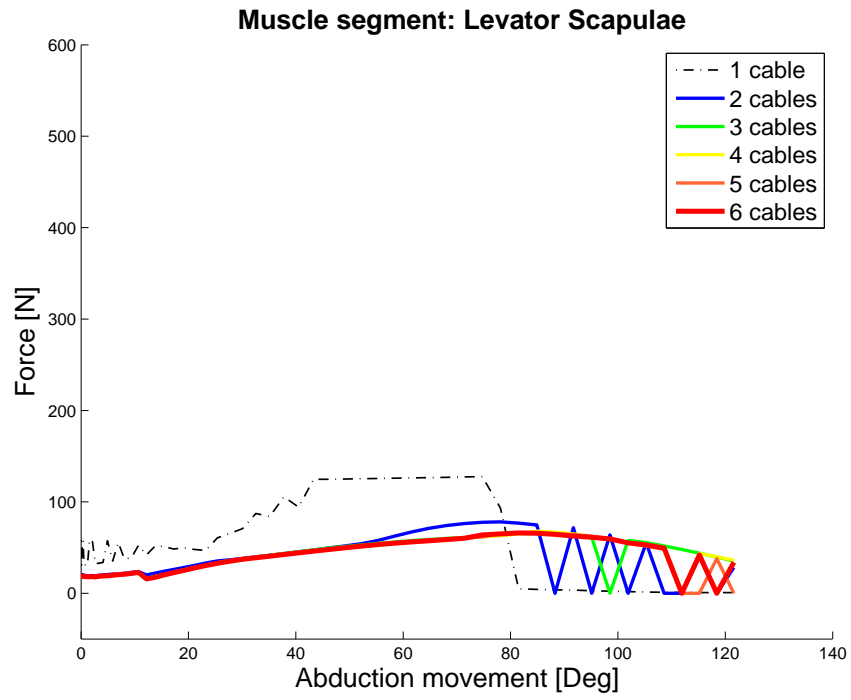
Figure B.8: Levator Scapulae
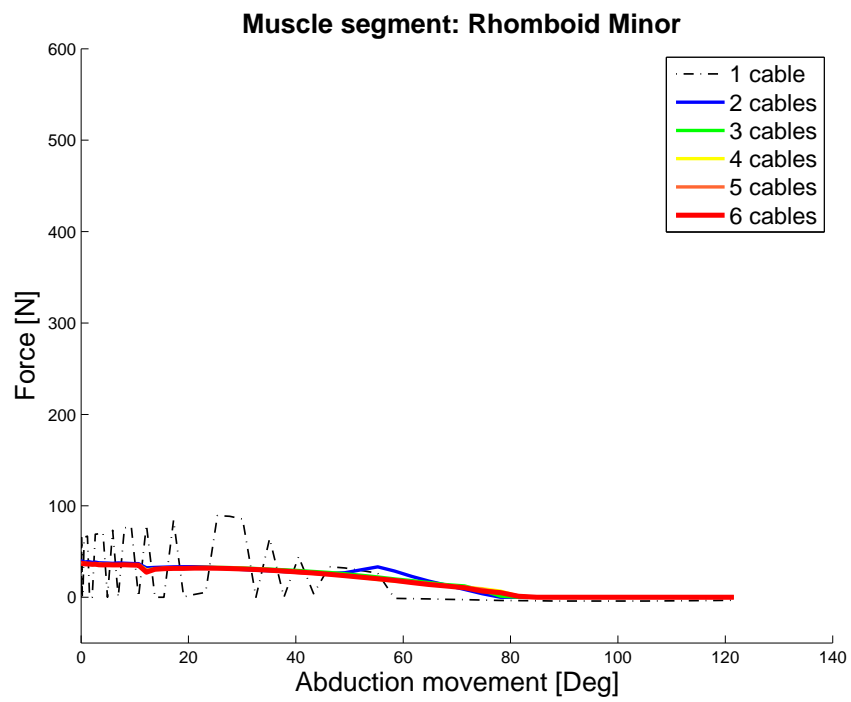
Figure B.9: Rhomboid Minor
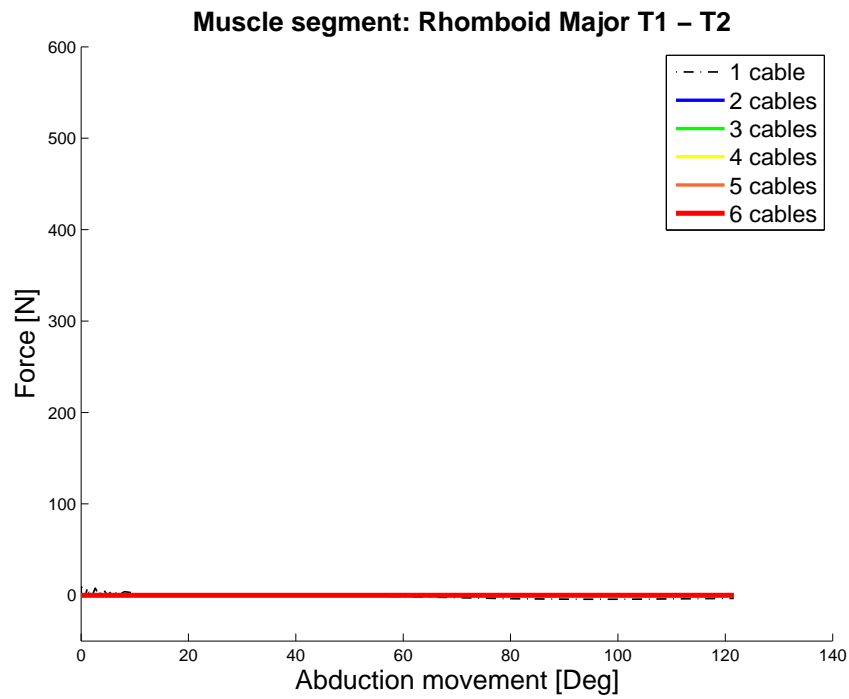
Figure B.10: Rhomboid Major T1-T2
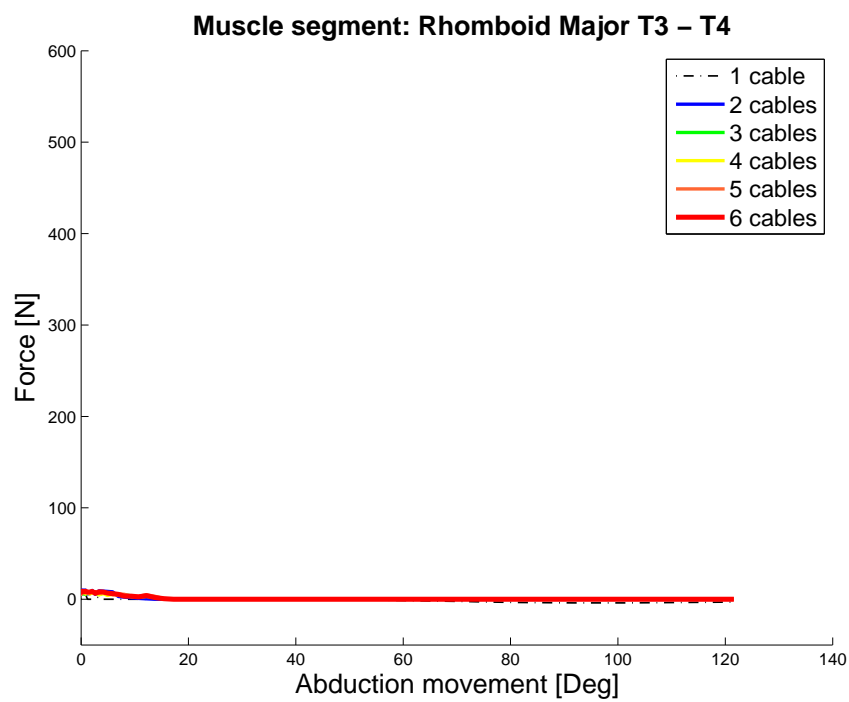
Figure B.11: Rhomboid Major T3-T4
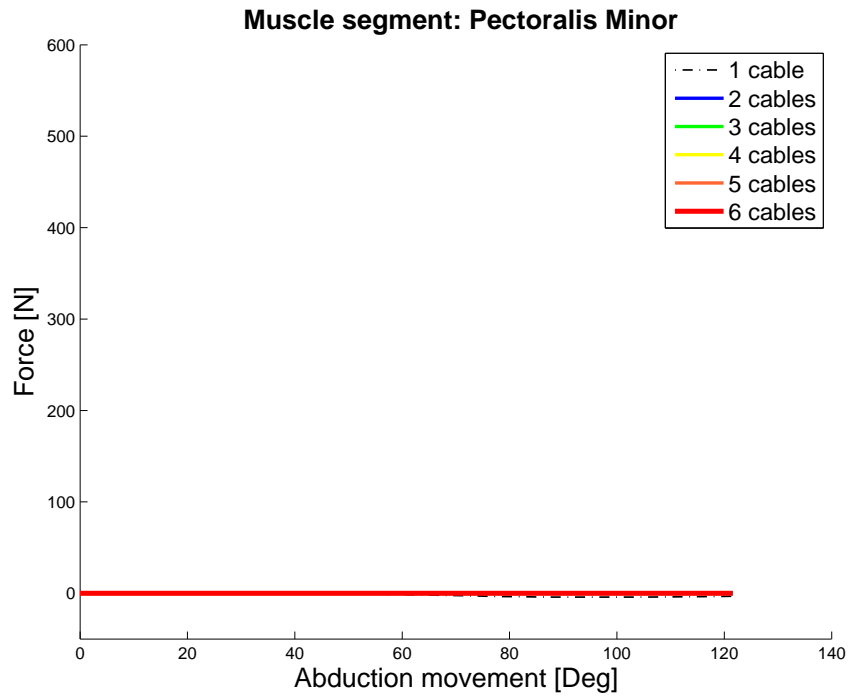
Figure B.12: Pectoralis Minor
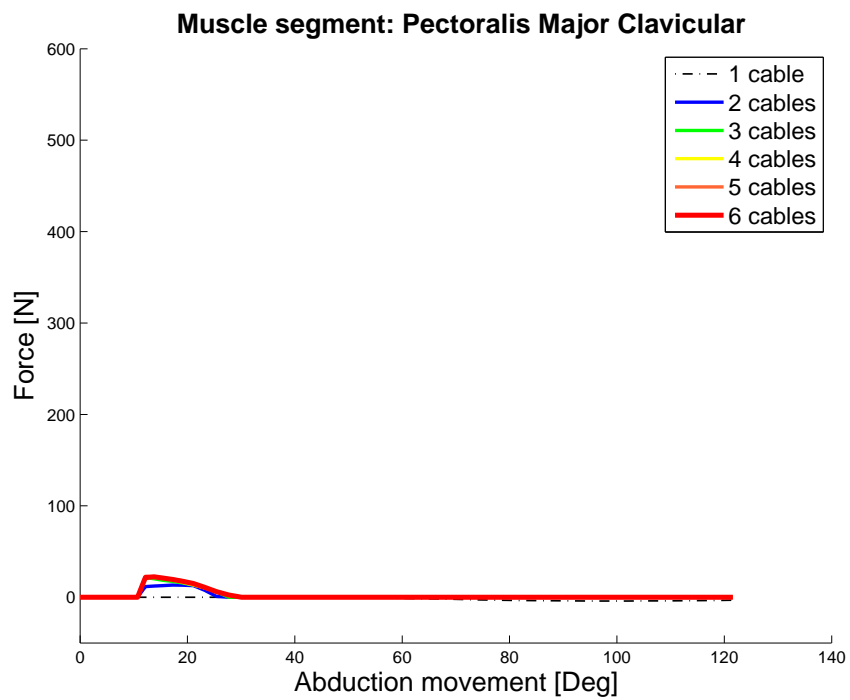
Figure B.13: Pectoralis Major Clavicular
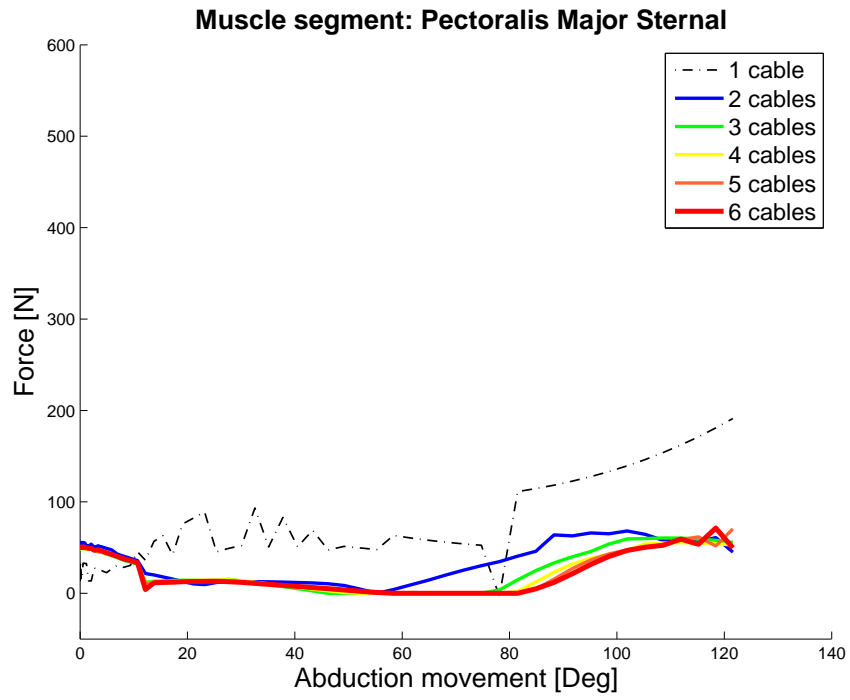
Figure B.14: Pectoralis Major Sternal
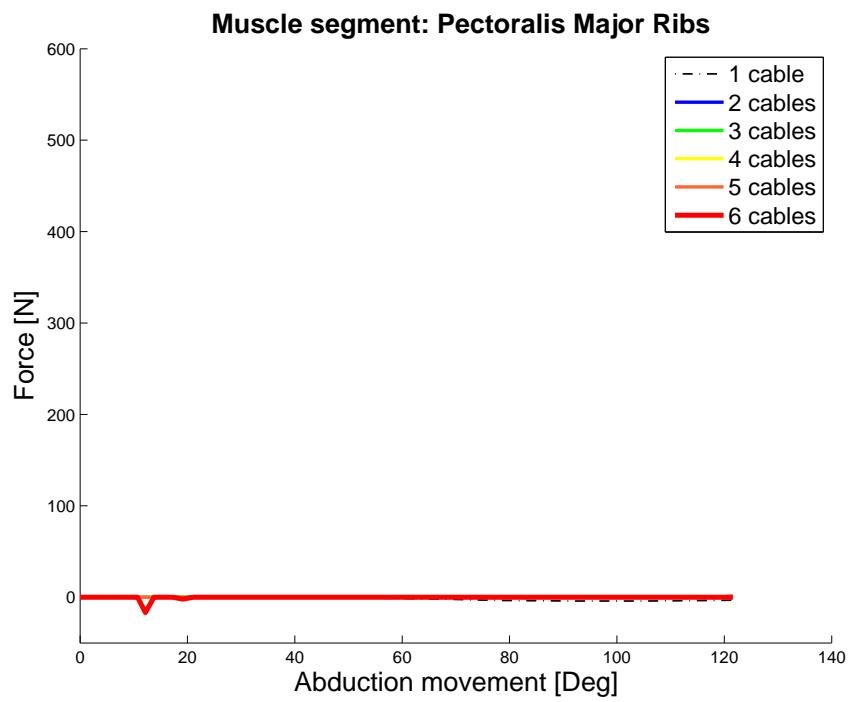
Figure B.15: Pectoralis Major Ribs
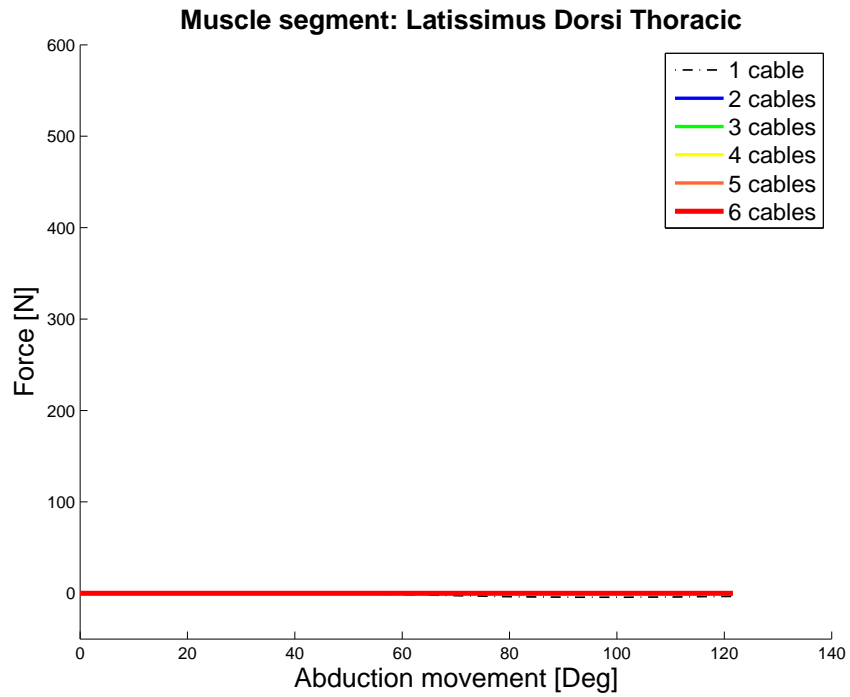
Figure B.16: Latissimus Dorsi Thoracic
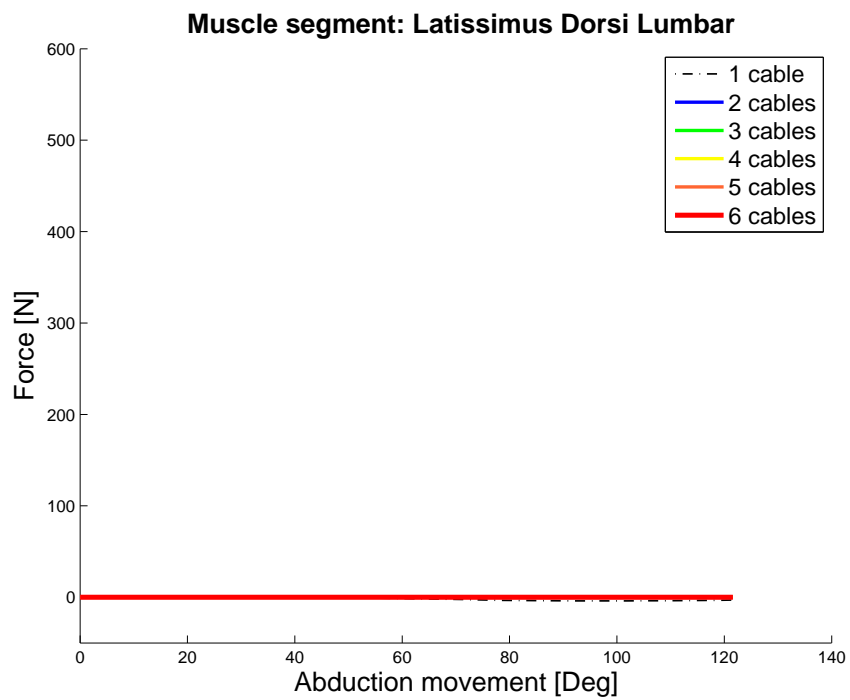
Figure B.17: Latissimus Dorsi Lumbar
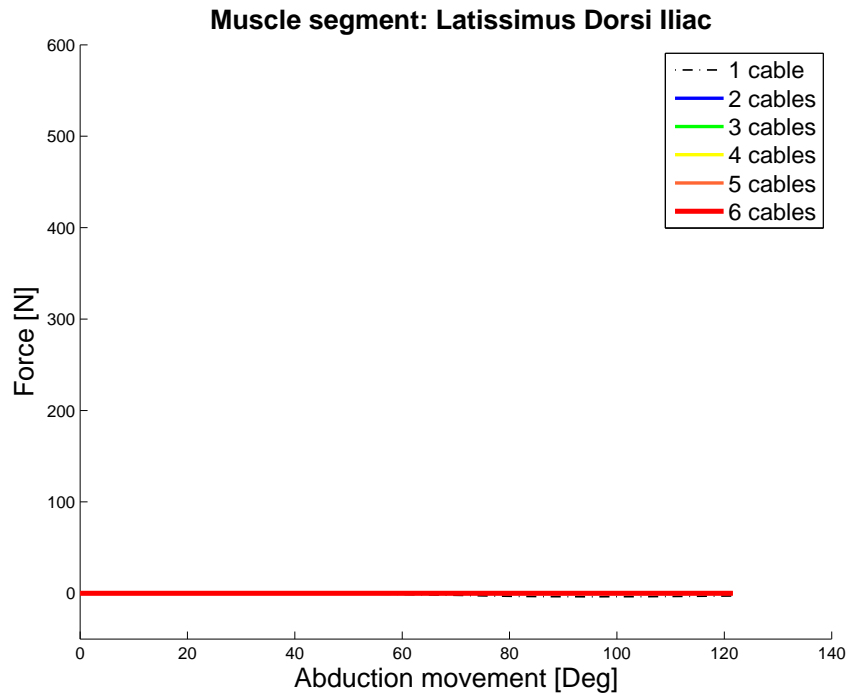
Figure B.18: Latissimus Dorsi Iliac
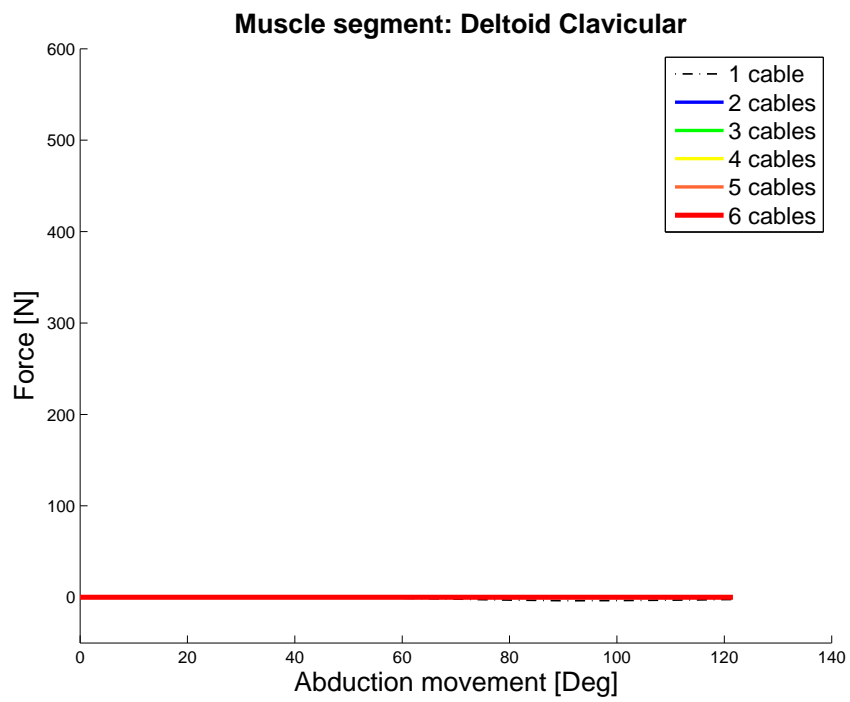
Figure B.19: Deltoid Clavicular

Muscle segment: Deltoid Scapular
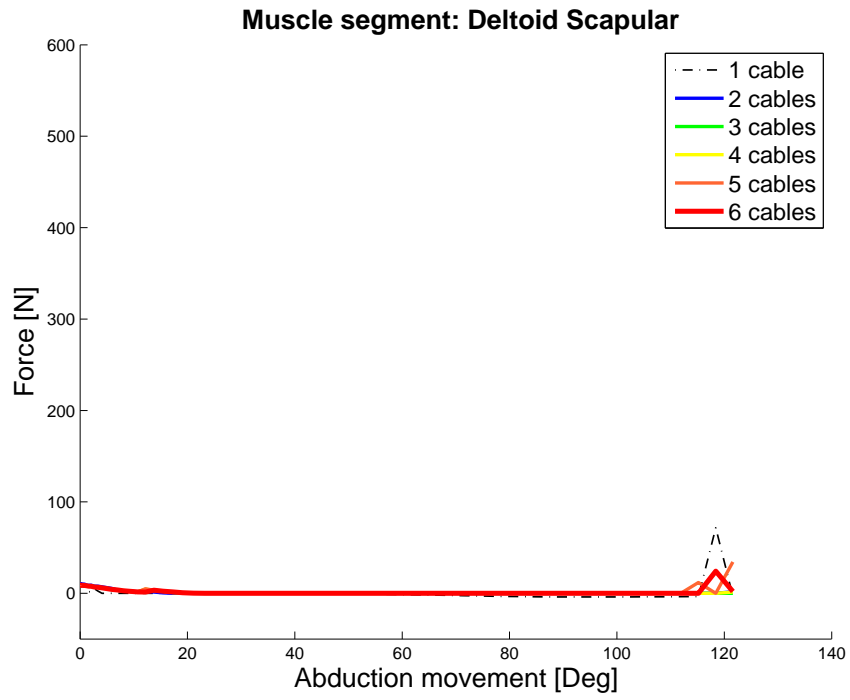
Figure B.20: Deltoid Scapular

Muscle segment: Infraspinatus
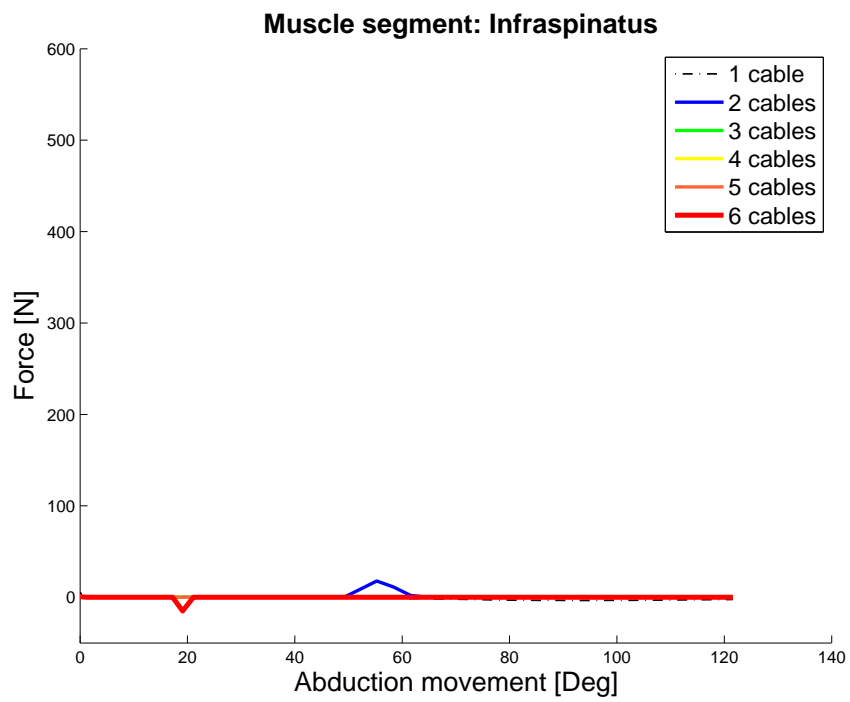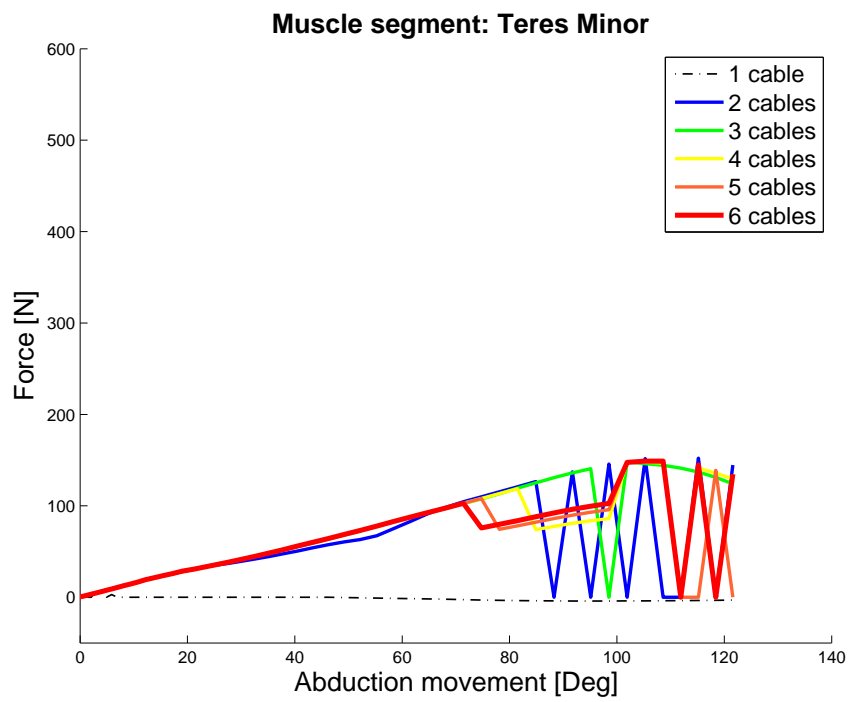

Figure B.21: Infraspinatus
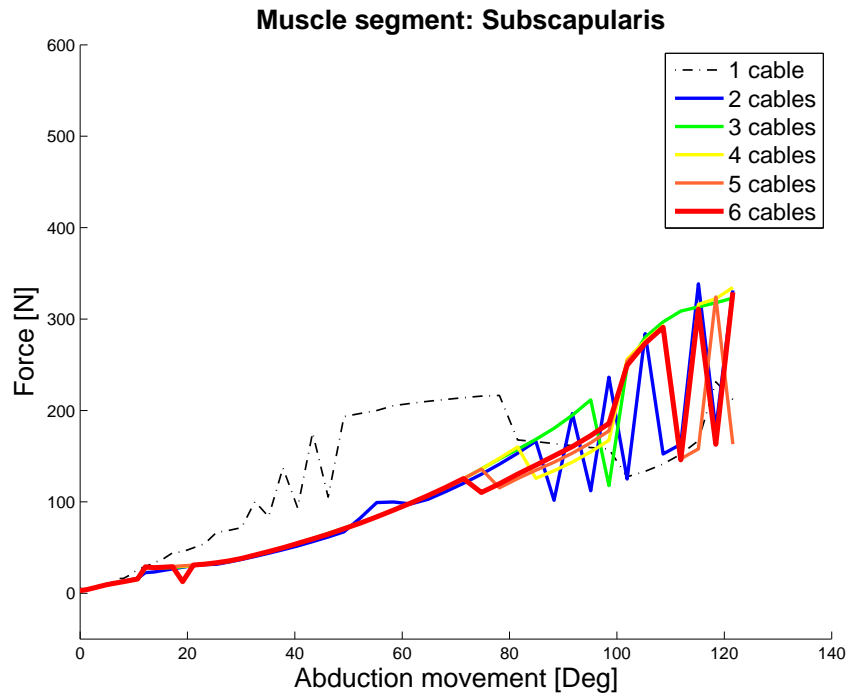
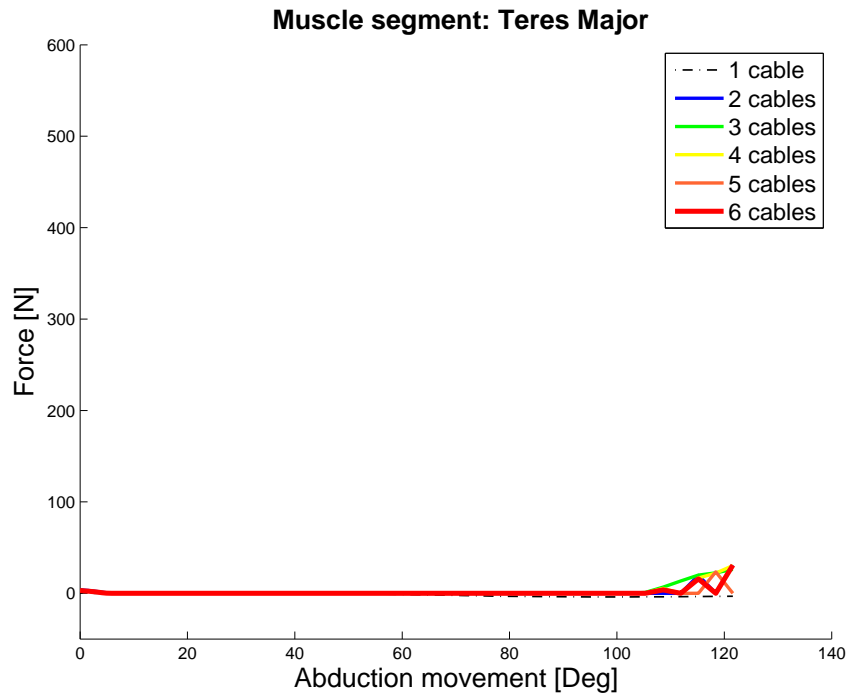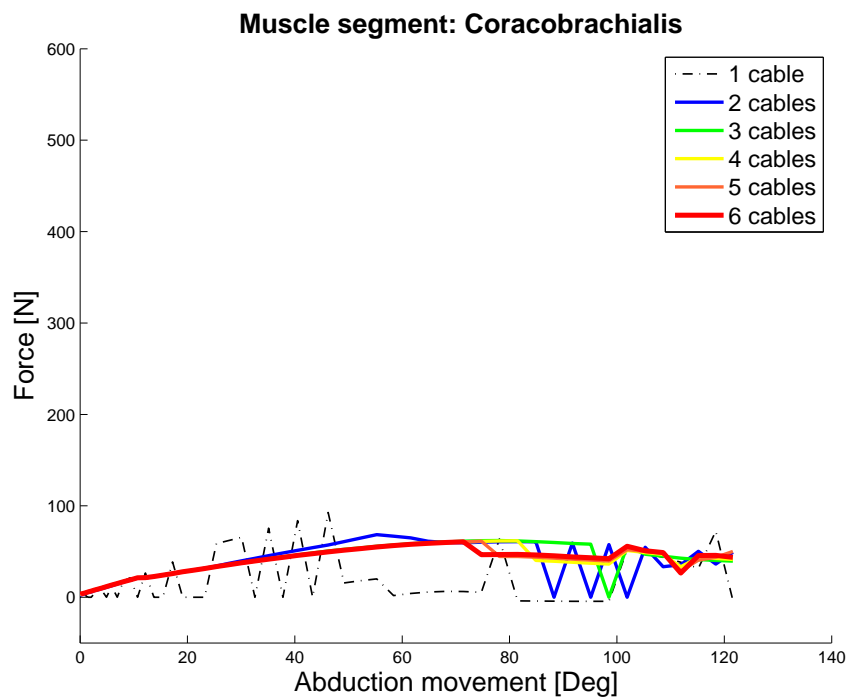Figure B.22: Subscapularis

Figure B.23: Teres Minor

Figure B.24: Teres Major

Figure B.25: Coracobrachialis